I. A Reinvestigation of the Vibration Spectra of Several Triatomic Molecules

II. The Infrared Spectrum and Configuration of Hydrogen Persulfide

III. Some Observations on the Spectrum of "Sulfur Monoxide"

Thesis

by

M. Kent Wilson

In Partial Fulfillment of the Requirements

for the Degree of

Doctor of Philosophy

California Institute of Technology

Pasadena, California

1949

Table of Contents

Page

Acknowledgments

Abstract i

I. A Reinvestigation of the Vibration Spectra of Several Triatomic Molecules 1

A. A Reinvestigation of the Vibration Spectrum of Ozone 2

B. A Reinvestigation of the Vibration Spectra and Configuration of Nitrogen Dioxide and Nitrogen Tetroxide 23

C. A Reinvestigation of the Vibration Spectrum of Oxygen Fluoride 47

D. Some Observations on the Vibration Spectrum of Sulfur Dioxide 59

E. Some Correlations between the Infrared Spectra and Structure of Several Triatomic Molecules 63

II. The Infrared Spectrum and Configuration of Hydrogen Persulfide 69

III. Some Observations on the Spectrum of "Sulfur Monoxide" 93

Appendix 115

References 120

Propositions

Acknowledgments

Acknowledgments

I should like to express my gratitude to Professor Richard M. Badger for his thorough instruction and understanding guidance during the period of my graduate study. I am also indebted to Dr. Oliver R. Wulf and Dr. Paul A. Giguère for their constant advice and assistance.

Grateful acknowledgment is made to Dr. Jerry Donohue for his calculations of the theoretical electron scattering curves for ozone.

I wish to extend my sincere thanks to all the members of the Gates and Crellin Laboratories of Chemistry, and in particular to Mr. William Schuelke and Mr. Trueman Robbins, for their helpfulness at all times.

Abstract

Abstract

The vibration spectra and molecular configuration of ozone and nitrogen dioxide have been the subject of considerable controversy. Part I of this thesis is a comparative study of the positions, relative intensities, and temperature dependence of the infrared absorption bands in the region 1.5-15 μ of ozone, nitrogen dioxide, oxygen fluoride, and sulfur dioxide.

The ozone band at 705 cm^{-1} is not temperature sensitive and, therefore, is not a difference band as was once postulated. The relative intensity of the ozone band at 2100 cm^{-1} is about that expected for a combination or overtone band and, therefore, this band need not be considered as a fundamental on the basis of intensity. A previously unreported band was found for ozone and has been shown to be the fundamental ν_1. A new assignment of fundamentals has been given which agrees with the positions, intensities, and contours of the observed ozone bands. In agreement with the electron diffraction results, this assignment requires an obtuse model for ozone. However, the rotational spacing observed in the perpendicular bands is only about one-half that calculated for the model found by electron diffraction.

The symmetric valence vibration, ν_1, for nitrogen dioxide previously had been unreported in the infrared, and conflicting assignments had been proposed for the observed nitrogen dioxide bands. By examining the spectrum of the nitrogen dioxide - nitrogen tetroxide system at 25° and 200° C, it was possible to locate the missing fundamental and to show that several of the bands previously ascribed to nitrogen dioxide are in reality nitrogen tetroxide bands. The symmetric valence vibration of nitrogen dioxide was found near 1306 cm^{-1} which is in good agreement with the value of 1320 cm^{-1} reported from measurements upon the temperature-sensitive ultraviolet bands. The rotational spacing observed in ν_2 for nitrogen dioxide is much smaller than that required by the molecular structure as determined by electron diffraction. If the existence of two identical overlapping bands is assumed, the spectroscopic and electron diffraction data can be reconciled. No explanation for the occurrence of two such overlapping bands can be given at this time.

Many of the bands previously assigned to oxygen fluoride have been shown to be due to an impurity, presumably carbon tetrafluoride. A new assignment of fundamentals has been given which accounts satisfactorily for the observed oxygen fluoride bands.

The apex angle decreases in the series, nitrogen dioxide - ozone - oxygen fluoride. It was observed that the values of ν_3, ν_3/ν_1, and the bond constant, K_1, also decrease while the interaction constant, K_{12}, increases. The value for the ozone bond constant seemed remarkably low in comparison with the value obtained for sulfur dioxide, but has now been shown to be intermediate between the bond constants of the more closely similar molecules, nitrogen dioxide and oxygen fluoride.

Heretofore the evidence has not been conclusive in support of either the plane symmetric or symmetric 90° model for nitrogen tetroxide. By new considerations involving the occurrence and frequencies of the N-O vibrations in nitrogen dioxide and nitrogen tetroxide, it has been possible to indicate that very probably the planes determined by the two NO_2 groups in nitrogen tetroxide are at 90° to each other.

Part II of this thesis is an investigation of the vibration spectrum of hydrogen persulfide and the rotational analysis of the band at 2μ. Since only one near-perpendicular type band and no near-parallel band could be investigated under high resolution, only the small moment of inertia was experimentally determined for the hydrogen persulfide molecule. Assuming a non-linear, non-planar (C_2) structure, it has been found that when the S-S distance, S-H distance, and S-S-H angle are allowed to vary within their range of probable values as inferred from the structures of similar molecules, the angle between the two S-S-H planes may be as small as 10° but no larger than 75° if the calculated least moment of inertia is to agree with observation. The maximum possible angle for hydrogen persulfide is somewhat smaller than the most probable angle in hydrogen peroxide.

The carrier of the absorption spectrum observed in a mixture of sulfur vapor and sulfur dioxide which has been passed through an electric discharge has variously been described as SO, S_2O_2, and S_2*.

The final part of the thesis describes several experiments undertaken in an attempt to identify the substance responsible for this spectrum. It was shown conclusively that oxygen is needed for the production of the spectrum, but that the absorption spectrum was not observed under conditions which yielded the SO bands strongly in emission. Although the necessity for the presence of oxygen appears to rule out S_2^* as the carrier, no decision could be made regarding the actual carrier of the spectrum.

Part I. A Reinvestigation of the Vibration Spectra of Several Triatomic Molecules

A. A Reinvestigation of the Vibration Spectrum of Ozone

1. Introduction

Several analyses of the vibration spectrum of ozone have been proposed in recent years (1,2,3,4,5) all of which have been open to serious objection. Either they have failed to account for the observed structure of all of the infrared bands or, if consistent with this structure, have required an acute angled molecular model which is not in accord with the structure determination by electron diffraction (6).

Since the previous assignments were partly based on arguments concerning the relative intensities (4,5) of the various ozone bands, it was indicated that even a roughly quantitative determination of the extinction coefficients would be of aid in arriving at the correct assignment of fundamentals. Further, an investigation of the temperature dependence of the ozone bands would aid in their identification by indicating the existence or absence of difference bands. At one time Simpson (4) suggested that the band at 705 cm^{-1} was a difference band rather than the fundamental ν_2. The following section of this thesis is concerned with the results of such a study of gaseous ozone.

2. Experimental procedure and results

Apparatus - The ozone spectrum was investigated from 1.5 - 15 μ with a Beckman IR-2 spectrophotometer. This prism instrument is equipped with rock salt optics and has a resolution of about 3 cm^{-1} at 9 μ. The wavelength drive can be motor driven and the output of the thermocouple connected to a Brown recorder to give a continuous plot of intensity versus wavelength. As intensity, rather than optical density, is plotted, it is necessary to determine the background periodically throughout a series of runs.

The ozone was prepared by passing specially pure tank oxygen (Linde Air Company) through the water-cooled Siemens-type ozonizer described by Johnston (7). Traps surrounded by dry ice were provided before and after the ozonizer to dry the oxygen and to condense small amounts of oxides of nitrogen which might have been produced (8) in the ozonizer from traces of nitrogen in the oxygen stream. A diagram of the gas system including the absorption cell is given in Figure 1.

The absorption cells were 50 and 100 cm in length by 3.1 cm in diameter with sodium chloride windows clamped in place as illustrated in Figure 1. The Koroseal gaskets used between the ground-glass surface and the rock salt windows were slowly attacked by ozone and, therefore, all observations were made with the ozone stream passing continuously through the absorption cell. In later experiments the Koroseal gaskets were replaced by gaskets fashioned from lead foil, but no other change was made in the technique.

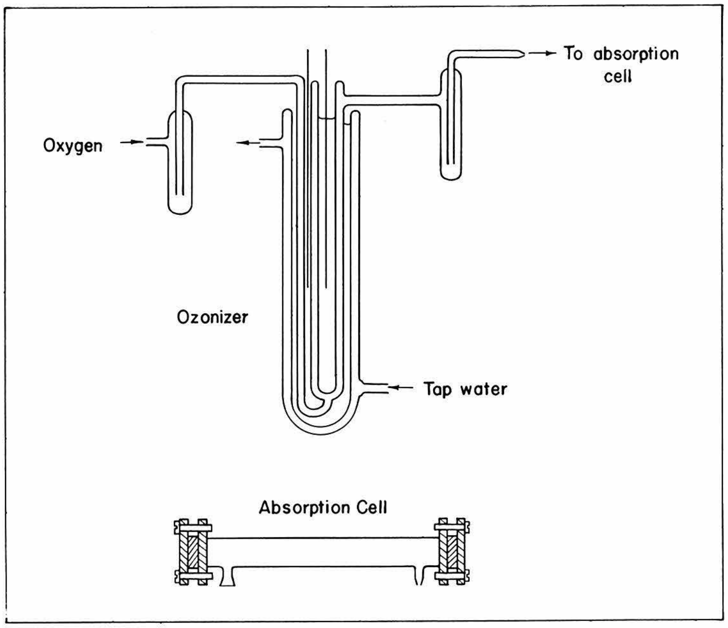

Figure 1. Ozone train and absorption cell

The standard taper joints were unlubricated.

Determination of absorption coefficients - The concentration of ozone in the gas stream was determined by absorbing the ozone from the gas stream in neutral potassium iodide solution and titrating the liberated iodine with thiosulfate solution (9). The volume of gas passed through the solution was calculated from measurements of the duration of flow, rate of flow, and total pressure. The rate of flow was determined before and after each absorption run by measuring the time necessary to displace 200 ml of water from an inverted 250-ml graduated cylinder. The flow rate and total pressure varied less than 3 percent during any determination.

If a spectrograph of infinite resolving power were available, the absolute intensity of an absorption band at any frequency could be obtained directly, since the instrument would measure I_0/I. With actual instruments it is the average integrated transmission over a more or less narrow band of frequencies that is measured. For bands which exhibit rotational fine structure the actual absorption may change drastically over narrow frequency ranges. Thus, the reading obtained with a low resolution instrument may deviate widely from the true absorption intensity. E. B. Wilson, Jr. and co-workers have recently reconsidered this problem (10). The true integrated absorption coefficient for unit pressure is defined as

$$A = \int \alpha \, d\nu = (1/pL) \int \ln I_0/I \, d\nu \qquad [1]$$

where L = path length
p = pressure
α = absorption coefficient /p

An apparent integrated absorption coefficient for unit pressure can be defined as

$$B = \int \beta \, d\nu' = (1/pL) \int \ln T_0/T \, d\nu' \qquad [2]$$

where T = the measured average transmission when the instrument is looking at a band of frequencies of which ν' is the midpoint

It is T in Equation [2] which actually is measured in low resolution spectrographs.

Wilson has shown that $\lim_{pL \to 0} B = A$ if the incident intensity does not vary rapidly over a slit width and if either the resolving power is high compared with variations in α or the resolving power does not change much over the band. Following Bartholomé (11) it was suggested that the extreme fluctuations of intensity caused by the rotational fine structure can be reduced by broadening the rotational lines by a sufficiently high pressure of a non-absorbing foreign gas. Thus, from measurements of the transmission over a band at various values of pL, the true integrated absorption coefficient can be obtained.

A similar procedure was applied to the ozone bands to determine α rather than A. Traces of the ozone spectrum were taken with various ozone partial pressures keeping the total pressure constant at 95 cm. Values of T_0/T were then taken from the traces at various positions across each band contour. For the weaker bands readings were taken at the maximum only. In Column 6 of Table 1 are tabulated values of $(1/pL) \ln T_0/T$ for given settings of the spectrograph. These values were then plotted as a function of pL and the resulting function extrapolated to zero pathlength. These extrapolated values then represent the average absorption coefficient at the position given. The values listed in Table 2 for each band are the average absorption coefficients for unit pressure near the maximum of each band. For ν_2, which shows ^PQ and ^RQ branches, the value given is the average value over the most intense region of the R branch. In Figure 2 the average absorption coefficients are plotted as a function of frequency.

Only for the bands at 1043 and 2105 cm^{-1} was it possible to arrive at a significant integrated absorption coefficient by the method employed by Wilson (10). The other bands were either not observed in their entirety (705 and 1110 cm^{-1}) or could not be observed with a sufficiently long pathlength to yield accurate measurements of T_0/T over the entire band. The integrated absorption coefficients for the 1043 and 2105 cm^{-1} bands are given in Table 3.

Table 1

Apparent Absorption Coefficients[a] of the Observed Ozone Bands for Several Ozone Partial Pressures

Ozone conc. (%)	d^b	14.5 μ Band				8.8 μ Band
		687 cm^{-1}	704 cm^{-1}	724 cm^{-1}	745 cm^{-1}	1125 cm^{-1}
		β^a	β	β	β	β
6.47	3.80	-	0.02	0.07	0.04	0.05
5.20	3.06	0.06	.03	.07	.04	.05
1.58	0.93	-	.01	.10	.04	.04

Ozone conc. (%)	d^a	5.7 μ Band 1750 cm^{-1}	4.7 μ Band 2124 cm^{-1}	3.6 μ Band 2800 cm^{-1}	3.3 μ Band 3050 cm^{-1}
		β	β	β	β
6.47	3.80	0.02	0.15	0.005	0.02
5.20	3.06	.02	.16	-	.01
1.58	0.93	.03	.15	-	.01

Ozone conc. (%)	d^a	9.5 μ Band	
		1057 cm^{-1}	1040 cm^{-1}
		β	β
0.41	0.24	4.3	2.8
.14	.082	5.4	3.2
.11	.065	5.7	3.5

[a] $\beta = (1/pL) \ln_{10} T_0/T$

[b] cm pure ozone at S.T.P.

Table 2

Apparent Absorption Coefficients[a] and Proposed Assignments of the Observed Ozone Bands

ν (cm^{-1})	Observed Type	Pred. Type	Spacing (cm^{-1})	Div.[b] (cm^{-1})	α[a]	Assignment
705	D	D	~5.7	-	0.07	ν_2
1043	Q	Q	~1	-	6.0	ν_3
1110	D	D	~5	-	0.05	ν_1
1740	?	Q	-	8	0.04	$\nu_2 + \nu_3$
2105	Q	Q	~1	48	0.15	$\nu_1 + \nu_3$
2800	?	Q	-	58	0.005	$\nu_1 + \nu_2 + \nu_3$
3050	Q	Q	-	79	0.015	$3\nu_3$

[a] α (base 10) is expressed as cm^{-1} of pure ozone at S.T.P.

[b] $(v_1\nu_1 + v_2\nu_2 + v_3\nu_3) - \nu_{obs.}$

Table 3

Integrated Absorption Coefficients for the 1043 and 2105 cm^{-1} Bands of Ozone

ν (cm^{-1})	A (cycles/sec.cm)
1043	660×10^{10}
2105	24×10^{10}

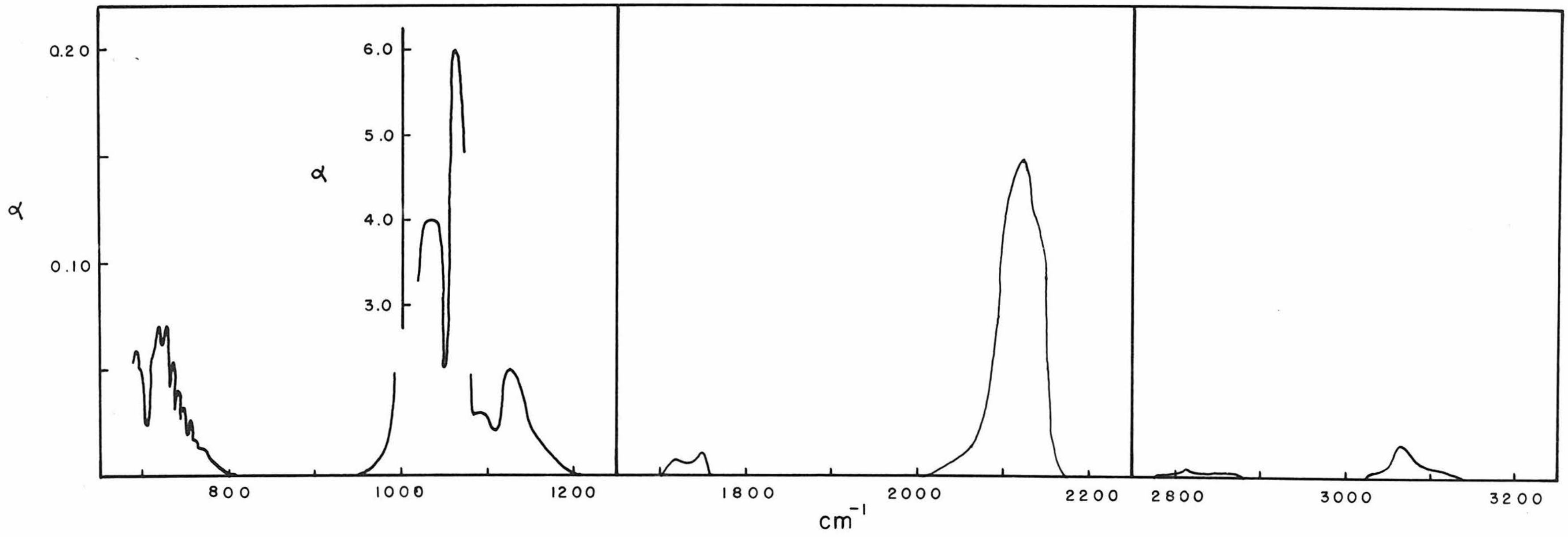

Figure 2. The observed infrared absorption spectrum of ozone under low dispersion; $\alpha = (1/pL) \log_{10} I_0/I$

The significance of these absorption coefficients in relation to the assignment of fundamental frequencies will be discussed later.

Temperature dependence of ozone bands - To investigate the temperature dependence of the ozone bands the spectrum was observed with the cell at room temperature and surrounded by dry ice. Only 44 cm of the 50-cm cell could be cooled to dry ice temperature without moisture condensing on the rock salt windows. Thus, the temperature of the cell was that of subliming carbon dioxide over 44 cm while the remaining 6 cm can be assumed to be at room temperature (25° C). Since only the change of absorption with temperature near the maximum of the bands was of interest, no analyses were made of the ozone content of the gas stream in these experiments. It had been determined previously that the rate of flow of oxygen through the system could be maintained essentially constant. Then for a given voltage impressed across the ozonizer, the ozone content of the gas stream remained unchanged throughout a set of measurements. When the cell was cooled in dry ice the amount of gas in the path was greater than it was at 25° C and, if there were no change in the extinction coefficient, the absorption would appear more intense at the lower temperature. However, this increase in intensity should be in the same ratio as the increase in the amount of material in the path. In Table 4 the increase in apparent average optical density near the maximum is given in Column 2, the increase of material in the path is listed in Column 3, and Column 4 contains the ratio of these two quantities. For bands which decrease in intensity with decrease in temperature, such as difference bands, this last column should be less than unity. It is seen that for all bands this ratio was slightly greater than unity. The apparent increase in absorption at the lower temperature can be explained in part by the change of band contour with temperature. At the lower temperature the band becomes narrower due to the decrease in population of the higher rotational levels and consequent increase in population of the levels nearer the band origin. Thus, for equal total absorption at the two temperatures, the value of ln T_o/T at the maximum will be larger at the lower temperature. This is observed in the ozone bands. It can then be concluded that none of the ozone bands observed in this investigation are difference bands.

Table 4

Effect of Temperature on the Apparent Absorption Coefficients of Ozone

Band	D_{206^o}/D_{298^o}	d_{206^o}/d_{298^o}	R[a]
14.5	2.06	1.39	1.48
9.5	1.80	1.39	1.29
8.8	2.05	1.39	1.47
5.7	1.44	1.39	1.04
4.7	1.44	1.39	1.04
3.6	1.90	1.39	1.37
3.3	1.70	1.39	1.22

[a] $R = D_{206^o}/D_{298^o} \div d_{206^o}/d_{298^o}$

3. Discussion

Assignment of the ozone bands - If ozone were in the form of an equilateral triangle, it would exhibit one non-degenerate infrared inactive fundamental vibration and one doubly degenerate infrared active fundamental vibration. It is not possible to explain the large number of bands observed on the basis of the equilateral model. The occurrence of binary combination bands of infrared active fundamentals rules out the possibility that the molecule is linear and symmetric. Binary combination bands of infrared active fundamentals are forbidden in molecules possessing a center of symmetry. The only models left to be considered are the non-linear symmetric structures having either an acute or obtuse apical angle. In both models all three fundamentals are infrared active. For the acute angled model the symmetric valence vibration, ν_1, and the deformation vibration, ν_2, yield an alternating dipole moment parallel to the least axis of inertia and, therefore, belong to the same symmetry class. These type A bands will exhibit a collected Q branch in addition to a P and R branch. For the asymmetrical valence vibration, ν_3, the dipole moment will be parallel to the intermediate axis of inertia and a type B band showing only a P and R branch (doublet) will result. In the acute angled model the C_2 axis is the axis of least moment of inertia. On the other hand, for the obtuse model the above conditions are reversed. Now the C_2 axis is the axis of middle inertia and both ν_1 and ν_2 produce an alternating dipole which is parallel to the C_2 axis. The dipole moment produced by ν_3 is then parallel to the least axis of inertia. Thus, for the obtuse model, ν_1 and ν_2 are doublets while ν_3 has the Q branch.

The assignment of fundamentals and the determination of the general shape of a non-linear symmetrical triatomic molecule is simple in principle -- first, locate the three fundamentals, and, second, determine their symmetry class. If two of the fundamentals have Q branches, the molecule has an acute apex angle. If only one band has a Q branch and two bands are doublets, the molecule is obtuse.

In ozone the problem has been mainly that of locating the three fundamentals. Recently there has been general agreement that both the bands at 705 and 1043 cm^{-1} had to be regarded as ozone fundamentals; although previously Simpson (4) had considered the 705 cm^{-1} band to be a difference band. This possibility is now definitely ruled out by the non-temperature dependence of this band as observed in the present investigation.

The particularly new observation made in the course of this work was the discovery of a new band with center at about 1110 cm^{-1} as shown in Figure 3(a). This band has nearly as great intensity as the fundamental at 705 cm^{-1}. It is suggested in several previously published tracings of the ozone spectrum but has apparently escaped special notice because of its proximity to the extremely intense band at 1043 cm^{-1}. Under conditions suitable for study of the latter band the former may easily escape detection. Although

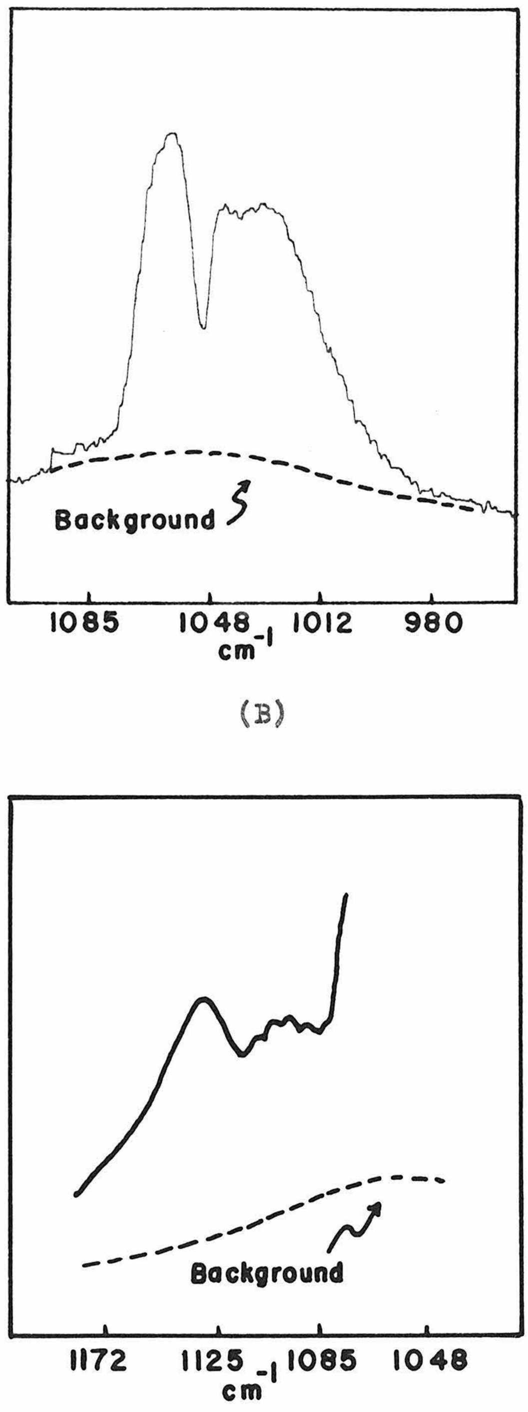

(A)

Figure 3. (B) The 1043 cm^{-1} band of ozone; equivalent pathlength = 0.10 cm

(A) The 1110 cm^{-1} band of ozone; equivalent pathlength = 11.3 cm these two bands overlap, substantially more than half of the $1110\ cm^{-1}$ band is visible. As shown in Figure 3(a), the new band shows no suggestion of a Q branch, but four maxima (presumably ^RQ branches) with an average spacing of about $5\ cm^{-1}$ have been resolved on the long wavelength side of the minimum. It seems reasonable to conclude that this new band is similar in structure to the fundamental at $705\ cm^{-1}$ which was found by Adel and Dennison to be a doublet with rotational spacing of $\sim 5.6\ cm^{-1}$. These two bands are to be described as ν_1 and ν_2, respectively. To investigate the possibility that the new band at $1110\ cm^{-1}$ might be due to nitrogen pentoxide the dry ice cooling was removed from around the traps and laboratory air drawn through the system. Although new bands did appear when nitrogen was present in the oxygen stream which passed through the ozonizer, no contamination occurred in the $1100\ cm^{-1}$ region.

The extremely intense band at $1043\ cm^{-1}$ must be a fundamental and, because it exhibits a Q branch, is ν_3. There has been some question as to the structure of this band, and it has been suggested that the observed fine structure is due in part to carbon dioxide contamination. This may be possible in observations of atmospheric absorption, but it is most unlikely under the laboratory conditions employed by Gerhardt (1). A tracing taken of carbon dioxide with a pathlength of 27 cm at one atmosphere pressure and 25° C showed no absorption in the $1050\ cm^{-1}$ region. The Q branch of the ozone band at 1043 cm^{-1} certainly is not prominent, but Figure 3(b) and, even more so, the tracings of Gerhardt, strongly suggest its presence, though somewhat displaced and "washed out" by convergence.

These new observations make possible the revised vibrational analysis presented in Table 2, which is in agreement with all observations on the band structures, and supports the approximate analysis of fine structure made by Miss Simpson (12) on the basis of the obtuse model. Table 5 gives the various assignments, the predicted band types, and a comparison of the calculated band position with the observed. In the assignment of Simpson as well as that of Penney and Sutherland the combination bands exhibit a divergence, while the assignment of Hettner, Pohlmann and Schumacher requires an acute angled model. In the present analysis these difficulties are now resolved. Table 6 gives the apparent absorption coefficients of the fundamentals of ozone and several similar obtuse triatomic molecules. In all cases ν_3 is found to be much more intense than ν_1. Therefore, the observed relative intensities of the bands support the proposed analysis. In particular, as is shown in Tables 2 and 3, the band at 2105 cm^{-1} is actually some 30 times less intense than the 1043 cm^{-1} band, rather than only two or three times less intense as previously supposed. The incorrect value for the relative intensity of these two bands apparently was the result of the misinterpretation of the tracing of Hettner, Pohlmann, and Schumacher (2). It is now evident that in this

Table 5

Various Proposed Assignments for the Observed Ozone Bands

ν (cm^{-1})	Observed type	Hettner, Pohlmann, and Schumacher (2) and Adel and Dennison (5)			Penney and Sutherland (3)		
		Assignment	Predicted type	Div.[a]	Assignment	Predicted type	Div.[a]
705	D	ν_3	D		ν_2	D	
1043	Q	ν_2	Q		ν_1	D	
1110	D	-	-		-	-	
1740	?	$\nu_2+\nu_3$	Q	8	ν_3	Q	
2105	Q	ν_1	Q		$2\nu_1;3\nu_2$	Q;D	-18;10
2800	?	$\nu_1+\nu_3$	Q	10	$2\nu_1+\nu_3$	Q	-12
3050	Q	$\nu_1+\nu_2$	Q	98	$3\nu_1$	D	79

ν (cm^{-1})	Observed type	Simpson (4)			Present Investigation		
		Assignment	Predicted type	Div.[a]	Assignment	Predicted type	Div.[a]
705	D	$\nu_1-\nu_2$	D	-8	ν_2	D	
1043	Q	ν_2	D		ν_3	Q	
1110	D	-	-		ν_1	D	
1740	?	ν_1	D		$\nu_2+\nu_3$	Q	8
2105	Q	ν_3	Q		$\nu_1+\nu_3$	Q	48
2800	?	$\nu_1+\nu_2$	D	-17	$\nu_1+\nu_2+\nu_3$	Q	58
3050	Q	$\nu_2+\nu_3;3\nu_2$	Q;D	98;79	$3\nu_3$	Q	79

[a] $(v_1\nu_1+v_2\nu_2+v_3\nu_3)-\nu_{obs.}$

earlier investigation about five percent of stray light was present at 10μ which made the 1043 cm^{-1} band appear much less intense than is the case.

Table 6

Comparison of the Apparent Absorption Coefficients of the Fundamentals of Several Triatomic Molecules

Band	SO_2(120°) β^a	NO_2(132°) β^a	O_3(127°) β^a	OF_2(100°) β^a
ν_1	0.30	0.05	0.05	0.002
ν_2	not observed	max. not observed	.05	not observed
ν_3	3.0	2.5	6.0	.17

[a] $\beta = (1/pL) \ln_{10} T_0/T$

It is of interest to compare the heat capacity of ozone calculated for the various assignments with the value reported by Lewis and von Elbe (13). On the basis of explosion data these investigators reported the average value of C_p for ozone between 300° and 476° K to be 10.94 ± .30 cals. With the present vibrational assignment the average value calculated for C_p is 10.29 cals. in the same temperature range. Although this is in better agreement than any previous assignment (see Table 7), the difference is rather large. Perhaps the observed value is somewhat high.

Table 7

Calculated Heat Capacity for Ozone in The Temperature Range 300° to 476° K for Various Assignments of Fundamentals

Fundamentals	Calculated Cp. Cals/deg.
1043, 1740, 2105	8.86[a]
710 , 1043, 2105	9.80[a]
710, 1043, 1740	9.89[a]
705, 1043, 1110	10.29[b]

Observed value of Cp = 10.94 ± .30

[a] See Reference (4)

[b] This value was calculated thus:

$$C_p = 8/2\,R + \sum_{i=1}^{3} \frac{R\left(\frac{hc\nu_i}{kT}\right)^2 e^{\frac{hc\nu_i}{kT}}}{\left(e^{+\frac{hc\nu_i}{kT}} - 1\right)^2}$$

where

ν_i = vibrational frequencies in cm^{-1}

The values of the calculated force constants for ozone in relation to those of several similar triatomic molecules will be discussed in Part I, Section E of this thesis.

The present assignment of fundamentals is in good agreement with all observations on the infrared spectrum of ozone but it is not in agreement with the published analyses of the ultraviolet bands (14,15,16). Eberhardt and Shand (16) concluded that it was "possible to ascribe almost all of the bands observed in the temperature-sensitive ultraviolet spectrum of ozone to the two fundamental frequencies 710 and 1043 cm^{-1}, and their harmonics and combinations". This observation strongly suggests that these two vibrations belong to the same symmetry class. In the analysis proposed here 705 cm^{-1} is a symmetric vibration while 1043 cm^{-1} is antisymmetric. It is not known whether a reasonable fit could have been obtained with the ultraviolet observations if the frequencies 705 and 1110 cm^{-1} had been tried.

Both vibrational analysis of the infrared bands proposed here and electron diffraction data require that ozone is in the form of an obtuse triangle. However, as Miss Simpson (4) pointed out, the structure as determined by Shand and Spurr ($O\text{-}O = 1.26 \pm 0.02$ A, $\measuredangle = 127 \pm 3^\circ$) requires the near perpendicular bands to exhibit a rotational structure with a separation of ~ 9.8 cm^{-1} as contrasted to the value of ~ 5 cm^{-1} as observed. The apex angle compatible with the O-O distance determined by electron diffraction and with the rotational spacing in the 705 cm^{-1} band is 102°, which is considerably outside the probable range permitted by the electron diffraction data. This 102° model would show a fine structure spacing in the near parallel bands of ~ 0.9 cm^{-1} which is approximately the value observed.

Theoretical intensity curves of electron scattering for ozone models with apical angles of 100°, 102°, and 104° and O-O bond distance of 1.26 A were calculated, but they show no resemblance to the curve for the 127° model of Shand and Spurr.

Even if the O-O bond distance is increased to 1.35 A, the apex angle is only decreased a few degrees if the least moment of inertia is to remain consistent with the spectroscopic data. Thus, although there is agreement on the general shape of the ozone molecule, the precise values of the apex angle and the internuclear distances are still in doubt. At present the rotational structure observed in ν_1 and ν_2 appears to be completely incompatible with the structure as determined by electron diffraction. In Part I, Section B of this thesis a similar situation is encountered in nitrogen dioxide and a possible solution to the difficulty is offered.

B. A Reinvestigation of the Vibration Spectra and Configuration of Nitrogen Dioxide and Nitrogen Tetroxide

1. Introduction

Although the infrared spectrum of nitrogen dioxide has been the subject of numerous investigations (see Herzberg (17)), there is still much doubt as to the correct assignment of fundamentals, in particular the location of the symmetric valence vibration, ν_1. Harris, Benedict, and King (18) from observations on the temperature-sensitive ultraviolet bands of nitrogen dioxide reported a value of 1320 cm^{-1} for ν_1. No band has previously been reported at this frequency in the infrared.

Since a recent electron diffraction investigation (19) has defined the structure of nitrogen dioxide within rather narrow limits ($O-N = 1.20 \pm .02$ A, $\sphericalangle = 132 \pm 3^o$), it seemed opportune to reinvestigate the vibration spectrum of this molecule. It may be noted that the non-linear triatomic molecules which have well-understood spectra have an apical atom which is much heavier than the other two atoms, for example: H_2O, H_2S, SO_2, etc. Both ozone and nitrogen dioxide contain three atoms of about equal mass and there has been much confusion concerning the spectra of both molecules. It was hoped that the elucidation of the vibration spectrum of nitrogen dioxide would be of aid in the ozone problem. Although this hope was not realized, it was possible to fix the location of ν_1, and to show that several of the infrared bands previously assigned to nitrogen dioxide actually are due to nitrogen tetroxide.

This work also afforded an opportunity to reinvestigate the spectrum of nitrogen tetroxide. The infrared and Raman spectra of nitrogen tetroxide have been extensively investigated (20,21,22,23) but the configuration of the molecule remains in doubt. Sutherland (23) considered the molecule to be symmetric and planar, but Harris and King (21) concluded it was impossible to decide between the planar and the symmetric 90° model on the basis of their spectroscopic data. Pauling (24) from electrostatic considerations suggested that an asymmetric model should be more stable than a structure having a bond between the two nitrogen atoms. We have been able to indicate from a consideration of the number and the relative positions of the N-O frequencies in nitrogen dioxide and nitrogen tetroxide that the tetroxide probably has the symmetric 90° structure.

2. Experimental procedure and results

Materials - Two separate samples of nitrogen dioxide were used in the present investigation. One sample was prepared by the decomposition of reagent grade lead nitrate which previously had been dried at 140° C for 10 hours. The dark green-blue color of the initial condensate indicated the presence of water, but after several distillations through phosphorous pentoxide the liquid had the yellow color characteristic of nitrogen dioxide free of nitric oxide and water. The second sample was prepared by drying tank nitrogen dioxide in a similar manner and storing the dry product over phosphorous pentoxide. No spectroscopic difference between the two samples was detected.

Apparatus - Spectra were taken from 1.5 to 15 μ with the Beckman IR-2 spectrophotometer with 5, 50, and 100-cm cells equipped with silver chloride windows sealed with Koroseal gaskets. The cells were wrapped with nichrome wire and lagged with asbestos cord in order that the temperature of the cell could be varied from room temperature to well above 200° C. The temperature of the cell was measured by a chromel-alumel thermocouple inserted in a well midway between the windows and between the heating coil and the glass wall of the cell. The temperature could be held constant to within ± 3° at 200° C.

Methods - The amount of material in the absorption cell was regulated by the temperature of the nitrogen dioxide in the trap connected by standard taper joints to the side arm of the absorption cell. With the trap immersed in a cooling bath of known temperature the stopcock between the evacuated cell and the trap was opened and kept open until equilibrium had been established -- a period of five to ten minutes. The establishment of equilibrium was determined by following the absorption at a particular wavelength as a function of time. The vapor pressure of the material in the trap was calculated from the following formulas taken from Yost and Russell (25):

Solid (m.p. 261.90° K)

$$\log_{10} p_{cm} = -2460.000/T + 9.58149 + 7.61700 \times 10^{-3}\ T - 1.51335 \times 10^{-5}\ T^2$$

Liquid (b.p. 294.25° K)

$$\log_{10} p_{mm} = -1753.000/T + 9.00436 - 11.8078 \times 10^{-4}\ T + 2.0954 \times 10^{-6}\ T^2$$

These equations refer to the equilibrium mixture of nitrogen dioxide-nitrogen tetroxide. Since at all times when filling the cell the trap was the coldest part of the system, the pressure calculated by the above equations also represents the pressure in the absorption cell. After the cell was filled at a given pressure, the stopcock on the side arm of the cell was closed and spectra taken at room temperature (25° C) and at 200° C with the same material in the path.

The partial pressures of nitrogen dioxide and nitrogen tetroxide in the cell were calculated at room temperature with the equilibrium constants reported by Verhoek and Daniels (26), and at 200° C with the aid of the data for ΔF^0 as given by Lewis and Randall (27). Table 8 contains the calculated total pressure for various temperatures of the nitrogen dioxide-nitrogen tetroxide mixture, and the partial pressures of both constituents at 25° C for each total pressure.

Table 8

Calculated Equilibrium Partial Pressures of Nitrogen Dioxide and Nitrogen Tetroxide for Various Total Pressures at 25° C [a]

P_T (cm)	P_{NO_2} (cm)	$P_{N_2O_4}$ (cm)
37.6	14.9	22.7
16.22	9.65	6.57
7.85	5.31	2.54
6.59	4.78	1.81
1.45	1.33	.12

[a] At 200° C the partial pressure of N_2O_4 was negligibly small at all except the highest pressure. At 200° C with a total pressure of 37.6 cm the partial pressure of N_2O_4 was .004 cm.

The absorption bands observed in this investigation were divided into two groups by the following method: the apparent average optical density ($D = \log_{10} T_0/T$) near the maximum was calculated for each band in nine sets of traces. Each set contained a trace at 25° C and one at 200° C with the same material in the path. For each band in each of the nine sets the ratio $D_{200^\circ}/D_{25^\circ}$ was formed. These data are tabulated in Table 9. All bands for which this ratio was zero were obviously tetroxide bands. At high total pressures in the absorption cell some of these bands did not quite disappear at 200° C, for a significant amount of nitrogen tetroxide was present at equilibrium. However, these bands could be made to disappear by decreasing the total pressure in the cell, and may with certainty be ascribed to the presence of nitrogen tetroxide. The bands for which nitrogen dioxide is the carrier showed values of the above ratio between 1.2 and 1.6 depending on the total pressure in the cell.

Table 9

Change of Intensity with Temperature of the Observed Nitrogen Dioxide - Nitrogen Tetroxide Bands

Band (cm^{-1})	$D_{200^\circ}/D_{25^\circ}$ [a]	Band (cm^{-1})	$D_{200^\circ}/D_{25^\circ}$ [a]
653	1.4	2605	0
750	.03 ; 0.00	2665	0
833	2	2750	0
1010	0	2900	1.4
1100	0	2965	0
1280	.05 ; 0.00	3120	0
1306	1.4	3450	0
1495	0	3545	1.2
1615	1.3	3570	0
1740	.05 ; 0.00	3990	0
1910	1.2	4230	1.4
1940	0	4250	0
1990	0	4330	.2 (?)
2070	0	4650	0
2130	0	4760	1.6
2220	0	4780	0
2290	0	5130	0
		5920	1.5

[a] $D = \log_{10} T_0/T$

Results - Table 10 includes the observed bands of nitrogen dioxide, the band assignment, and the approximate apparent absorption coefficients near the maximum of each band. Table 11 contains the nitrogen tetroxide bands observed in the present investigation. The values listed for the apparent average absorption coefficients, with the exception of those for the 1280 and 1740 cm^{-1} bands, were determined only roughly and indicate little more than the relative intensities of the bands. Traces taken at 25° C and 200° C with the same amount of material in the cell are reproduced in Figure 4. Figure 5 contains a plot of intensity versus frequency for the observed nitrogen dioxide bands.

Table 10

Absorption Coefficients and Assignments for the Observed Nitrogen Dioxide Bands

ν (cm^{-1})	β^a	Assignment	Band type	Div.^{b}
653	-	ν_2	doublet	
833	.04	$\nu_3 - \nu_2$		164
1306	.05	ν_1	doublet	
1615	2.5	ν_3	Q	
1910	.005	$\nu_1 + \nu_2$		10
2900	.15	$\nu_1 + \nu_3$		22
3545	.005	$\nu_1 + \nu_2 + \nu_3$		40
4230	.005	$2\nu_1 + \nu_3$		0
4760	.001	$3\nu_3$		85
5920	.0005	$3\nu_3 + \nu_1$		202

[a] $\beta = (1/pL) \ln_{10} T_0/T$

[b] Div. $= (v_1\nu_1 + v_2\nu_2 + v_3\nu_3) - \nu_{obs.}$

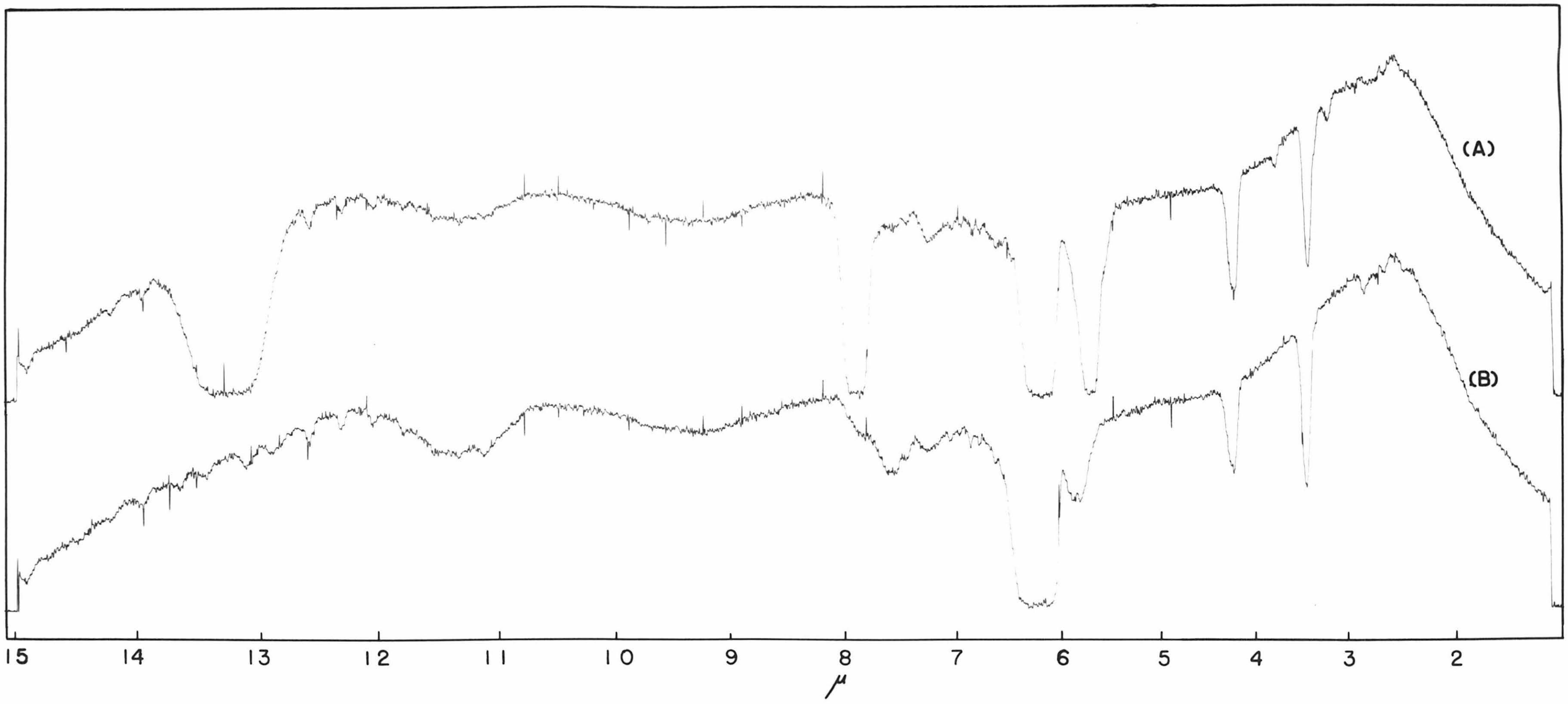

Figure 4. (A) The nitrogen dioxide - nitrogen tetroxide bands at 25° C; equivalent pathlength ≈ 2.54 cm

(B) The nitrogen dioxide - nitrogen tetroxide bands at 200° C; equivalent pathlength ≈ 2.54 cm

Figure 5. The observed infrared absorption spectrum of nitrogen dioxide under low dispersion; $\beta = (1/pL) \log_{10} T_0/T$

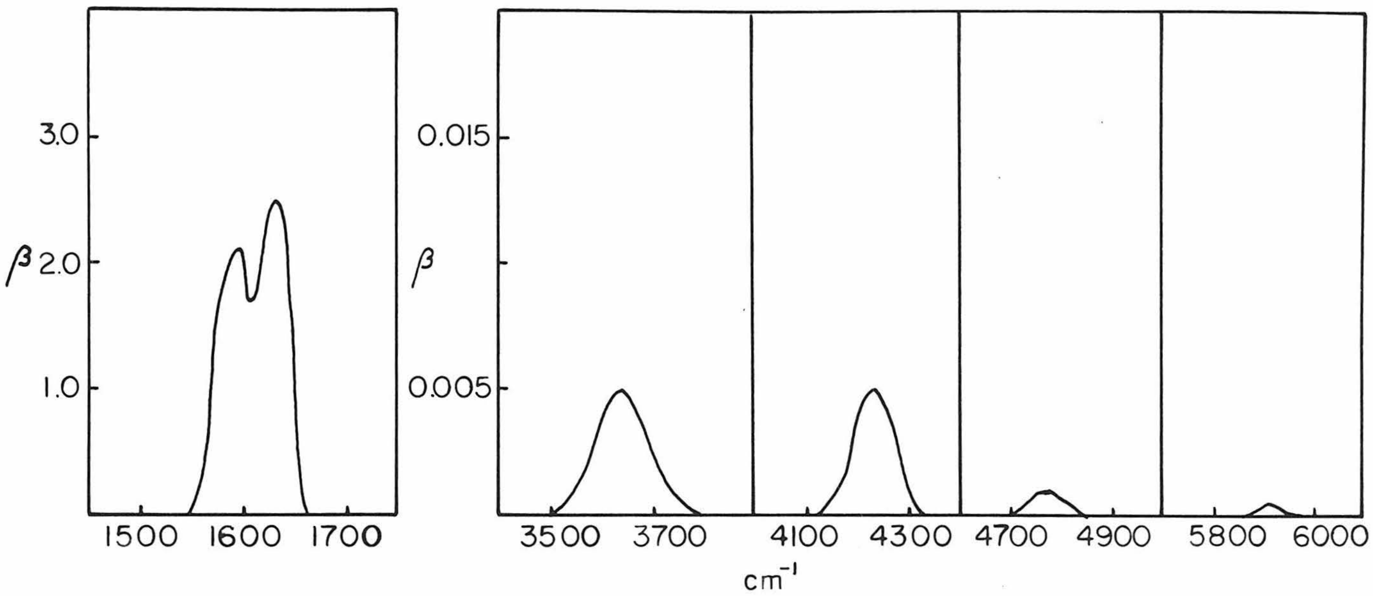
3.0
β 2.0
1.0
1500
1600
1700
0.015
β
0.005
3500
3700
4100
4300
4700
4900
5800
6000
cm^{-1}

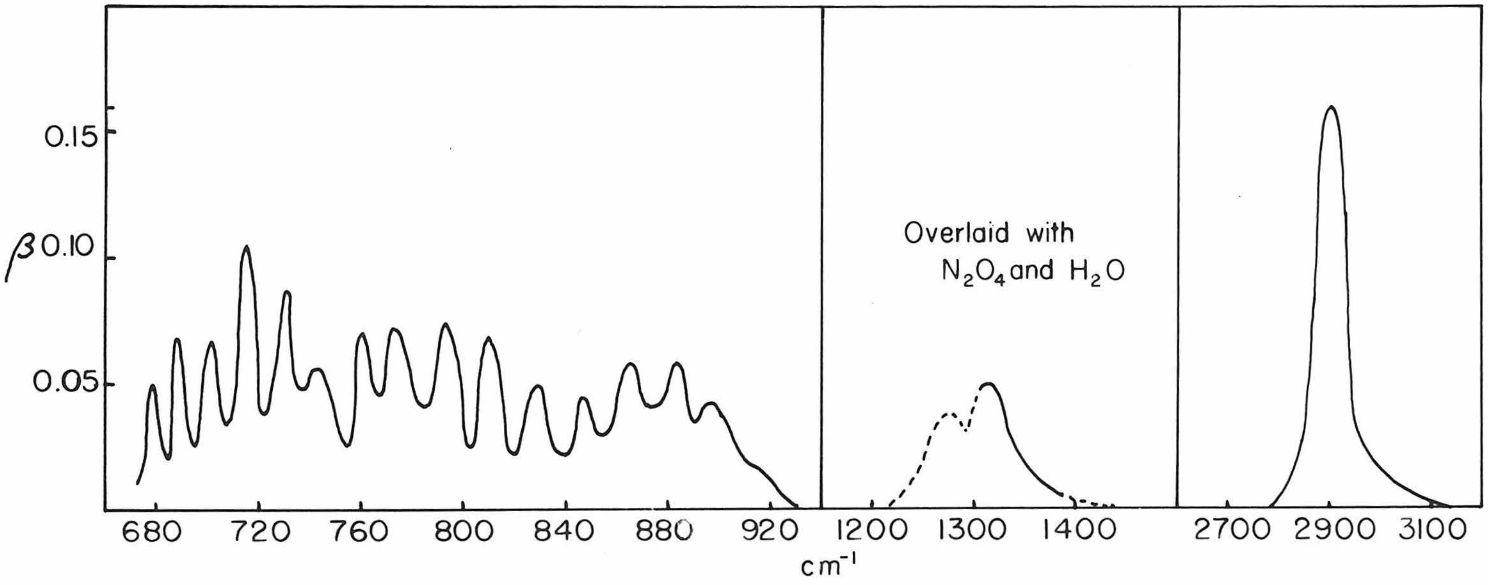
0.15
β 0.10
0.05
680
720
760
800
840
880
920
1200
1300
1400
2700
2900
3100
cm^{-1}
Overlaid with
N_2O_4 and H_2O

3. Discussion

(a) Nitrogen dioxide

On the basis of the obtuse model for nitrogen dioxide the assignment given in Table 10 can be made. The fundamental ν_1 which previously had been unreported in the infrared was found at 1306 cm^{-1}. This is very close to the position (1320 cm^{-1}) which had been predicted from observations made on the ultraviolet bands of nitrogen dioxide (18). As can be seen in Figure 4, this comparatively weak band lies very close to the extremely intense tetroxide band at 1280 cm^{-1}. Even with very small amounts of the tetroxide in the path the absorption of the 1280 cm^{-1} band is almost strong enough to mask this nitrogen dioxide fundamental.

The assignment of fundamentals given in the present investigation is identical with that reproduced by Herzberg (17), but it now seems likely that some of the bands listed by Herzberg do not belong to nitrogen dioxide. Table 12 lists the dioxide bands as given previously and in Table 11 are tabulated the tetroxide bands observed in the present investigation. A comparison of Tables 11 and 12 shows that the bands listed by Herzberg at 1000, 2220, 2605, 2665, 3930, 4140, and 4560 cm^{-1} actually are tetroxide bands. The band at 3240 cm^{-1} was described by Harris and King (21) as having no maximum. This band was not observed for either nitrogen dioxide or nitrogen tetroxide in the present investigation. The weak band at 1373 cm^{-1} reported for nitrogen dioxide conceivably could be due to compound formation on the windows. Williams and Derchard (28) report that the nitrate ion exhibits a band at 1370 cm^{-1}.

Table 11

The Infrared Spectrum of Nitrogen Tetroxide as Observed in the Present Investigation

ν (cm^{-1})	β^a	ν (cm^{-1})	β^a	ν (cm^{-1})	β^a
750	2.5	2070	0.001	3120	0.05
1010	.02	2130	.004	3450	.02
1100	.003	2220	.002	3570	.002
1280	3.0	2290	.003	3990	.001
1495	.02	2605	.002	4250	.005
1740	4.0	2665	.05	4330	.0005
1940	.01	2750	.001	4650	.003
1990	.006	2965	.1	4780	.002
				5130	.001

[a] $\beta = (1/pL)\ \ln_{10} T_0/T$ near the most intense portion of the band

Table 12

Previous Assignments for the Nitrogen Dioxide Bands (17)

ν (cm^{-1})	Assignment	ν (cm^{-1})	Assignment
648	ν_2	2910	$\nu_3 + \nu_1$
1000	$\nu_3 - \nu_2$	3240	$2\nu_3$
1320^a	ν_1	3454	$\nu_1 + \nu_2 + \nu_3$
1373	$(2\nu_2\ ?)$	3597	
1621	ν_3	3930	?
2220	$\nu_3 + \nu_2$	4140	$2\nu_1 + \nu_3$
2601	$2\nu_1$	4560	$\nu_1 + 2\nu_3$
2667		4753	$3\nu_3$

[a] From ultraviolet bands

The calculated position of the band at 833 cm^{-1} is unsatisfactory, but there seems little doubt that it belongs to nitrogen dioxide as it showed no tendency to decrease in intensity when the temperature of the gas was increased. Its contour and exact temperature behavior are uncertain since it was overlaid by the extensive nitrogen dioxide band with center reported at 648 cm^{-1}.

Both symmetrical vibrations ν_1 and ν_2 were observed to exhibit rotational structure in the R branch. In neither ν_1 nor ν_2 could the P branch be investigated. The P branch of ν_2 was outside the region accessible to the spectrophotometer, and for pressures which gave sufficient absorption for ν_1 enough nitrogen tetroxide was present to cause the P branch of the nitrogen dioxide band to be masked by the tetroxide band at 1280 cm^{-1}. Tables 13 and 14 contain the positions of the observed ^RQ sub-bands in ν_2 and ν_1, respectively. The values given for ν_2 are the average of those obtained from four separate traces, while three traces were measured to arrive at the values given for ν_1. As discussed in Section A, for both ν_1 and ν_2 of an obtuse triatomic molecule the alternating dipole is perpendicular to the axis of least inertia. The spacing between the sub-bands in perpendicular bands is related to the least moment of inertia. If the molecule were a symmetric top and the moments of inertia in the lower and upper state were equal, the sub-bands would be evenly spaced at a distance of $A''-B''$. Nitrogen dioxide is not quite a symmetric top and the moments of

Table 13

Rotational Structure of 653 cm^{-1} Band of Nitrogen Dioxide

Sub-Bands (cm^{-1})	$\Delta\nu$ (cm^{-1})	Scheme A m	Scheme A $\nu-\nu_0/m$[a]	Scheme B m	Scheme B $\nu-\nu_0/m$[b]
679	10	2.5	10.4	1.5	17.4
689	13	3.5	10.3	2.5'	18.8
702	14	4.5	10.9	2.5	19.6
716	15	5.5	11.5	3.5'	21.2
731	12	6.5	12.0	3.5	22.3
743	18	7.5	12.1	4.5'	22.5
761	12	8.5	12.7	4.5	24.0
773	20	9.5	12.7	5.5'	23.8
793	17	10.5	13.3	5.5	25.5
810	19	11.5	13.7	6.5'	25.8
829	21	12.5	14.1	6.5	27.1
848	17	13.5	14.4	7.5'	27.4
865	18	14.5	14.6	7.5	28.3
883	15	15.5	14.9	8.5'	28.4
898	20	16.5	14.9	8.5	28.8
918		17.5	15.2	9.5'	29.1
$A''-\frac{1}{2}(B''+C'')$		4.5 cm^{-1}		6.2 and 6.7 cm^{-1}	

[a] $\nu_0 = 653$ cm^{-1}

[b] $\nu_0 = 653$ cm^{-1} for unprimed terms and 642 cm^{-1} for primed terms

Table 14

Rotational Structure of 1306 cm^{-1} Band of Nitrogen Dioxide

Sub-Bands (cm^{-1})	$\Delta\nu$ (cm^{-1})	m	$\nu-\nu_0/m$[a]
1313	14	.5	14.0
1327	17	1.5	14.0
1344	15	2.5	15.2
1359	13	3.5	15.1
1372	15	4.5	14.7
1387	14	5.5	14.7
1401	16	6.5	14.6
1417	16	7.5	14.8
1433		8.5	15.0

$A''-\frac{1}{2}(B''+C'') = 7.4$

[a] $\nu_0 = 1306$ cm^{-1}

inertia depend on the vibrational state, but the positions of the sub-bands can be approximated by the following formula:

$$\nu_{\text{sub-bands}} = \nu_0 + \left[(A'-B') \quad (A''-B'')\right] m + \left[(A'-B') - (A''-B'')\right] m^2$$

where A = least moment of inertia
B = one-half the sum of the two larger moments of inertia
m = 1/2, 3/2, ---

or

$$(\nu - \nu_0)/m = \left[(A'-B') + (A''-B'')\right] + \left[(A'-B') - (A''-B'')\right] m$$

If $(\nu - \nu_0)/m$ is plotted as a function of m, a straight line results whose intercept is $(A'-B') + (A''-B'')$ and whose slope is $(A'-B') - (A''-B'')$. Since the molecule is slightly asymmetric, the lines near the origin will be somewhat displaced and, because the spacing actually depends also upon higher terms in m, the curve will deviate from a straight line at high m values.

The center of the band near 650 cm^{-1} could not be observed in the instrument employed, consequently both ν_0 and the numbering of the bands are in doubt. A reasonable numbering system and value for ν_0 is listed in Table 13 and plotted in Figure 6. When all the sub-bands were included in one numbering system (Scheme A), a value of 4.5 cm^{-1} was obtained for $(A''-B'')$ as compared to 6.8 cm^{-1} calculated for the structure as determined by electron diffraction (19). However, if the sub-bands were ordered in two groups as indicated in Scheme B, values of 6.2 and 6.7 cm^{-1} were found for $(A''-B'')$. A similar treatment for ν_6 (Table 6 and Figure 3) yielded a value of

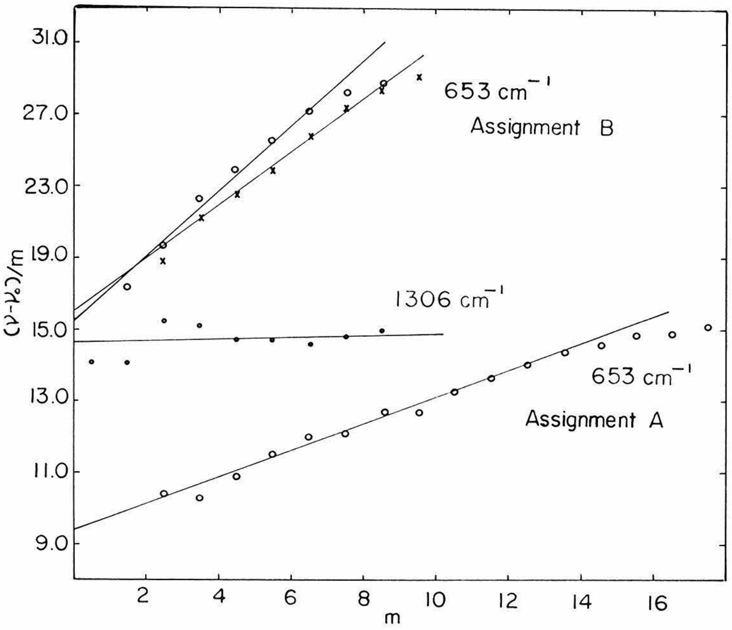

Figure 6. Determination of $(A''-\frac{1}{2}(B''+C''))$ for the ν_1 and ν_2 bands of nitrogen dioxide

7.4 cm^{-1} for (A"-B") when all the sub-bands were ordered in one system.

In Section A it was pointed out that the observed spacing between consecutive sub-bands in ν_2 for ozone did not agree with that calculated for the structure given by electron diffraction. It appears that in both ozone and nitrogen dioxide the spectroscopic data for ν_2 can be brought into agreement with the electron diffraction structure by assuming the presence of two overlapping bands. At the present time no satisfactory explanation for the occurrence of two overlapping bands in ν_2 can be given for these nonlinear-triatomic molecules.

(b) Nitrogen tetroxide

If the NO_2 groups are at 90° to each other in nitrogen tetroxide, the molecule is an exact symmetric top and belongs to point group V_d. For this structure the twelve fundamentals will yield nine distinct bands: three doubly degenerate vibrations active in both Raman and infrared, three vibrations Raman active only, two non-degenerate vibrations both Raman and infrared active, and one vibration inactive in both Raman and infrared. The band contours of a symmetric top fall into two classes; either they exhibit a collected Q branch in the center of the band in addition to a P and R branch, or they exhibit only a single maximum. For a planar asymmetric top molecule the parallel bands would have a Q branch but the perpendicular bands would exhibit a doublet structure. Sutherland (23) investigated several of the tetroxide bands under medium dispersion with a grating instrument in an effort to determine

Pages 39, 40, 41, and 42 have been deleted from this thesis. Therefore, Table 15 and References 29, 30, 31, and 32 do not appear in the text.

the band contours. He concluded that the 1740 cm^{-1} band was a doublet and, therefore, the 90° structure was eliminated. His published spectrum is badly contaminated by water vapor and hence the purported doublet structure does not appear too convincing. Sutherland investigated the Raman spectrum of solid nitrogen tetroxide and found shifts of 28, 57, 79, 283, 500, 813, 1337, 1382, and 1724 cm^{-1}. The first three values he considered to be too low to correspond to vibrational frequencies and assigned them to restricted rotations in the crystal. The other six bands presumably are vibration frequencies of the tetroxide molecule.

Consider the occurrence of Raman and infrared N-O bands in the planar and 90° model (see Figure 7). The planar model has a center of symmetry and thus no vibration occurs in both the Raman and infrared. The asymmetric valence vibration in nitrogen dioxide appears as one Raman active and one infrared active vibration in nitrogen tetroxide. In the Raman active vibration the nitrogen atoms move in opposite directions in the plane. This has the effect of introducing an additional force constant into this vibration and, therefore, the Raman line would be expected to lie higher in frequency than the infrared active vibration in which the two oscillators are coupled. In the 90° model this asymmetric vibration is doubly degenerate and is both Raman and infrared active. The observed Raman line which must be ascribed to the asymmetric valence vibration is found at a slightly lower frequency than the infrared band (1724 cm^{-1} as compared to 1740 cm^{-1}).

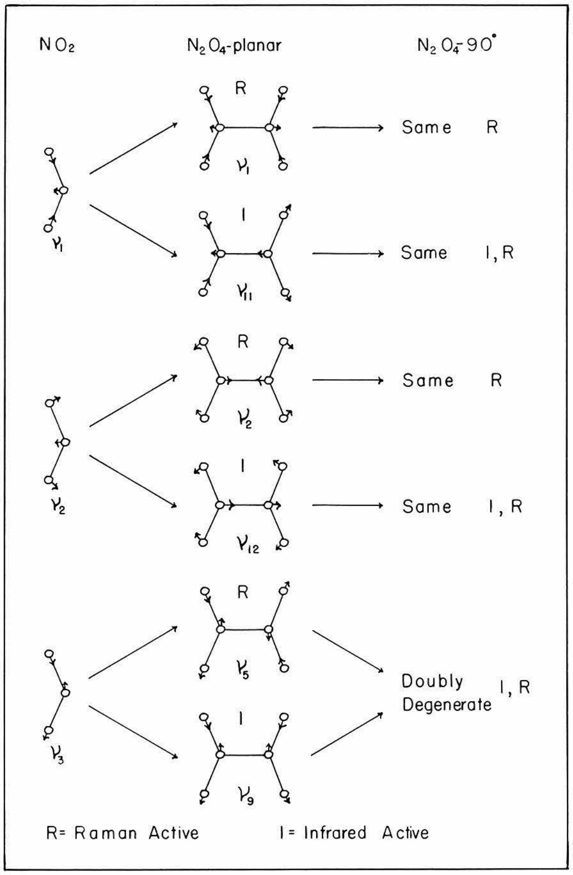

Figure 7. Form of the normal vibrations in nitrogen tetroxide corresponding to those in nitrogen dioxide

Accordingly, this Raman line is more easily explained with the 90° model than with the planar structure.

In the plane-symmetric model for nitrogen tetroxide there occurs two vibrations corresponding to the symmetric N-O vibration in nitrogen dioxide: one Raman active and one infrared active. However, the 90° model should yield one Raman active and one active both in the Raman and infrared. Raman lines of about equal intensity were found at 1337 and 1382 cm^{-1} in solid nitrogen tetroxide. Sutherland considered them actually to be one line which had been split by resonance degeneracy. These lines may also be explained as the two Raman active symmetric N-O frequencies of the 90° model. The band at 1337 cm^{-1} should correspond to the infrared active band at 1280 cm^{-1}. Although the difference between 1280 and 1337 cm^{-1} is very large, it may not be too large to be explained as the difference between the spectrum of the solid and the gas. The 90° model predicts the existence of eight Raman lines, while the planar requires only five. The fact that as yet only six have been observed may mean that two of the Raman lines are relatively weak.

It may be important that the Raman spectrum of nitrogen tetroxide was obtained from the solid. If the potential barrier for rotation around the N-N bond is small, it may be that the configuration of the tetroxide is different in the solid than it is in the gas. This possibility has been discussed by Wu (33).

The asymmetric structure  proposed by Pauling remains to be discussed. No normal coordinate treatment of this structure has been given, nor can the various force constants be approximated at this time. It is, therefore, difficult to estimate the number and position of the vibrations which might be classified roughly as N-O vibrations. It seems probable that this structure should show at least three infrared active N-O vibrations, but the intensity relationships are unknown. Since this is a highly unsymmetrical molecule it is probable that all twelve fundamentals would appear more or less strongly in the infrared. Also, the lack of symmetry would predict that the Raman shifts would be weak. The nitrogen tetroxide molecule shows a very intense Raman line at 283 cm^{-1} , and the number of bands that can be considered as fundamentals which are found in the infrared are relatively few. Thus, the spectroscopic evidence favors, but does not prove, a symmetric structure which is not planar.

The nitrogen tetroxide bands observed in this investigation are listed in Table 11. Due to the uncertainty which still exists concerning the configuration of the tetroxide molecule, it does not seem profitable to attempt an assignment of these bands.

It appears that a final decision regarding the nitrogen tetroxide configuration must be delayed until the infrared band contours have definitely been established.

C. A Reinvestigation of the Vibration Spectrum of Oxygen Fluoride

1. Introduction

Several electron diffraction investigations have been made of oxygen fluoride (34,35,36), and Boersch (34) concluded that the molecule is in the form of an obtuse triangle with apical angle of $100 \pm 3^{\circ}$ and O-F bond distance of $1.41 \pm .05$ A. Only one investigation of the infrared spectrum of this interesting compound has been reported (37).

An inspection of the published absorption curves of Hettner, Pohlmann, and Schumacher (37) indicated that the infrared spectrum of oxygen fluoride might be explained by an assignment of fundamentals very similar to that which had been found applicable to ozone in Section A of this thesis. The fluorine used in the previous oxygen fluoride preparation was generated with the use of graphite electrodes and, therefore, contained some carbon tetrafluoride. The authors considered that the oxygen fluoride preparation used in the spectroscopic investigation contained about one or two percent carbon tetrafluoride and oxygen. Since even a small amount of carbon tetrafluoride might cause serious contamination of the infrared spectrum of oxygen fluoride, it appeared worth while to redetermine the spectrum of oxygen fluoride before attempting a new vibrational assignment.

2. Experimental procedure and results

Materials and methods - Oxygen fluoride was prepared after the manner described by Lebeau and Damiens (38). Tank fluorine (manufactured by Pennsylvania Salt Co.) was bubbled slowly through a two-percent aqueous solution of potassium hydroxide which was continuously renewed. After emerging from the potassium hydroxide solution, the gas stream was passed through two traps immersed in a dry ice - methanol mixture to condense water and then into a trap cooled in liquid air. This last trap condensed essentially all of the oxygen fluoride (b.p. -144.8° C) as well as some oxygen which is also produced in the reaction. The apparatus is illustrated in Figure 8.

Pure liquid oxygen fluoride is described as possessing an intense yellow-orange color. The product as condensed in liquid air was light yellow presumably due to the presence of considerable oxygen. To free the product of oxygen the trap was kept in liquid air and evacuated by means of a water aspirator. As the oxygen was removed, the material in the trap deepened in color. After about one-third of the liquid had been volatilized, the volume of the residue diminished only slowly and no further color change could be detected. This material was then used for the infrared study without further purification.

The oxygen fluoride spectrum was taken with a 100-cm cell in the Beckman IR-2 spectrophotometer. The cell was fitted with silver chloride windows made vacuum tight with Koroseal gaskets. It was

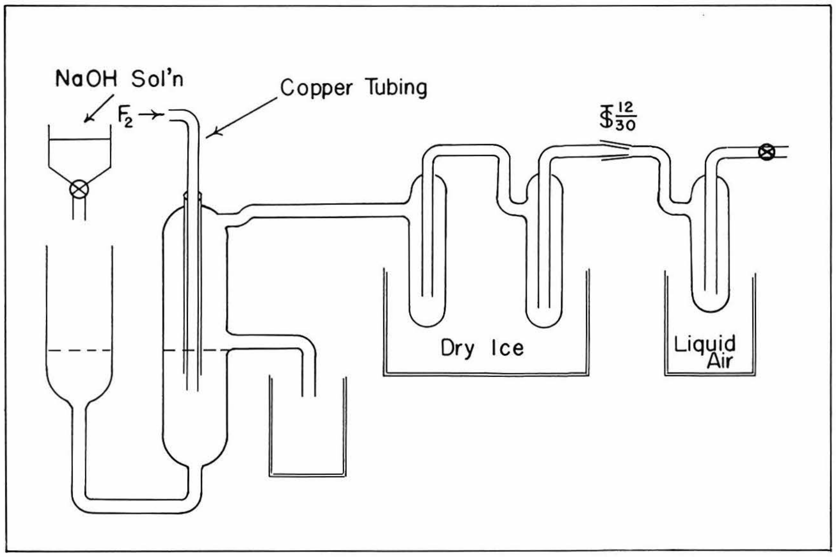

Figure 8. Apparatus for the preparation of oxygen fluoride

observed that oxygen fluoride reacted with the silver chloride windows and Koroseal gaskets to yield volatile substances as well as compounds which adhered very strongly to the windows. Although the absorption bands due to these substances were bothersome, they could not be mistaken for oxygen fluoride bands. The compounds formed on the windows persisted when the cell was evacuated, and the bands due to volatile reaction products increased in intensity with the length of time the oxygen fluoride remained in the cell. The behavior of these spurious bands can be seen in Figure 9.

The temperature dependence of the oxygen fluoride bands - As an aid in the assignment of fundamentals, the temperature dependence of the oxygen fluoride bands was investigated between -80° and 150° C. The cell was filled at 25° C and a trace taken. The cell was then packed with dry ice and, after waiting for 20 minutes for temperature equilibrium to be established as indicated by the thermocouple reading, the low-temperature trace was taken. The dry ice was then removed and the temperature of the cell increased to 150° C by electrically heating the lagged coil surrounding the cell. After the high temperature trace had been taken, the cell was allowed to cool to room temperature and the 25° C trace repeated. As indicated in Figures 9 and 10, the band at 723 cm^{-1} was the only oxygen fluoride band which showed an appreciable dependence upon temperature. As will be discussed later, this band can be described as a difference band having as its lower state the low frequency deformation vibration and as its upper state the band at 1240 cm^{-1}.

Figure 9. (A) The oxygen fluoride bands at 25° C

(B) The oxygen fluoride bands at -80° C

(C) The oxygen fluoride bands at 150° C

(D) The oxygen fluoride bands at 25° C

The spectra were taken in the order given with the same material in the cell for all traces. The bands which increase in intensity with time are due to reaction products of oxygen fluoride with the Koroseal gaskets or with the silver chloride windows.

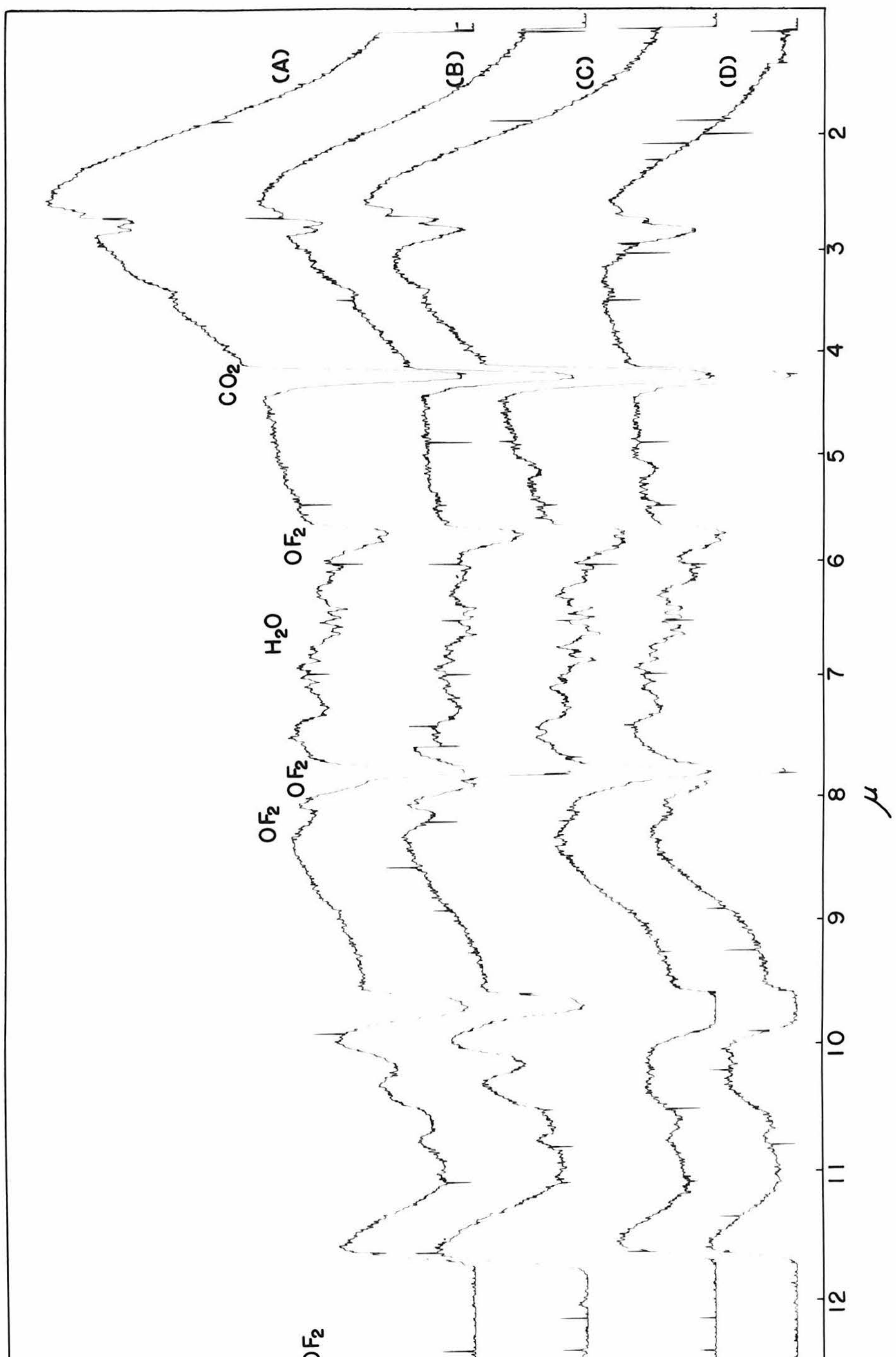
(A)
(B)
(C)
(D)
CO_2
OF_2
H_2O
OF_2
OF_2
OF_2
OF_2
CO_2
2
3
4
5
6
7
8
9
10
11
12
13
14
15
μ

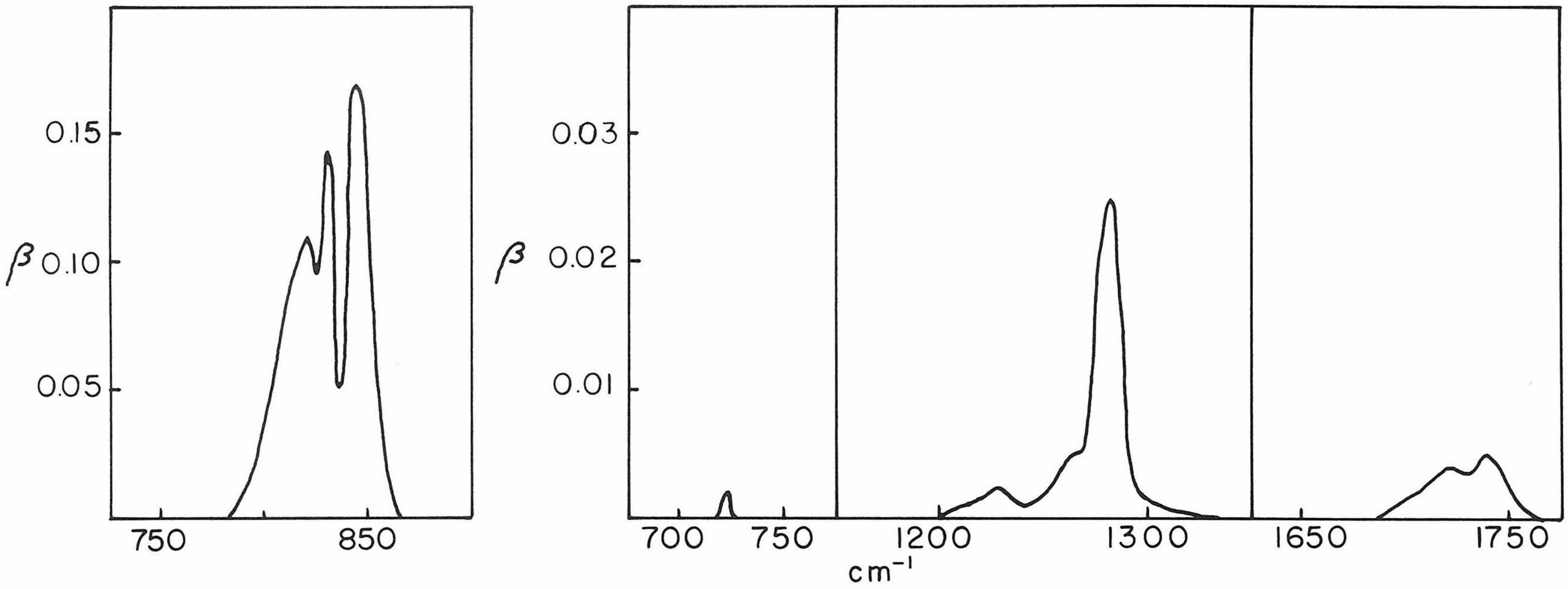

Figure 10. The observed infrared absorption spectrum of oxygen fluoride under low dispersion; $\beta = (1/pL) \log_{10} T_0/T$

Accepting the obtuse symmetric model indicated by electron diffraction, the assignment given in Table 16 can be made. Also included in the table are approximate apparent absorption coefficients for the observed bands. Since the pressure in the cell and the amount of oxygen in the oxygen fluoride were known only approximately, the coefficients given indicate merely the order of magnitude of the apparent average absorption near the maximum. They also serve to indicate the relative intensities of the bands. Figure 10 is a plot of $(1/pL) \log_{10} T_0/T$ against frequency.

3. Discussion

Figure 11(a) is a reproduction of the oxygen fluoride spectrum as published by Hettner, et. al. (37). A comparison of this trace with Figure 10 shows that the previous workers found many more bands than were observed in the present investigation. The two assignments which they considered probable are given in Table 16 as well as the assignment proposed by Sutherland and Penney (39) from the Hettner, Pohlmann, and Schumacher data. Although Hettner, et. al. considered several of the bands they observed to be due to carbon tetrafluoride, the later work of Bailey, Hale, and Thompson (40) (see Table 17 and Figure 11(b)) on the carbon tetrafluoride spectrum indicates that the contamination of the oxygen fluoride spectrum was more extensive than was originally suspected. A comparison of the two spectra and the oxygen fluoride bands found in the present work shows that the bands observed by Hettner, et. al. at 625, 926, 1110, 2190, and 2544 cm^{-1} very probably were the same bands that

Table 16

Various Proposed Assignments for the Observed Oxygen Fluoride Bands

ν	Present Investigation				Hettner, Pohlmann, and Schumacher (37)		Sutherland and Penney (39)
(cm^{-1})	Observed type	Assignment	β^a	Div.^{b} (cm^{-1})	Assignment I	Assignment II	Assignment
517^c	-	ν_2	-	-	d	d	ν_2
625	-	-	-	-	d	d	$\nu_3 - \nu_2$
723	(?)	$\nu_1 - \nu_2$	0.002	c	-	-	-
828	Q	ν_3	.17	-	ν_1	-	ν_1
926	-	not observed	-	-	ν_2	ν_1	$2\nu_2$
1110	-	not observed	-	-	d	d	ν_3
1240	D	ν_1	.002	-	-	-	-
1282	(?)	$\nu_2 + \nu_3$	.02	95	ν_3	ν_2	$\nu_1 + \nu_2$
1740	D	$\nu_1 + \nu_2$	.005	17	$\nu_1 + \nu_2$	ν_3	$\nu_1 + 2\nu_2$
2190	-	not observed	-	-	$\nu_2 + \nu_3$	d	$2\nu_3$
2544	-	not observed	-	-	$2\nu_3$	$2\nu_2$	$2\nu_1 + 2\nu_2$

[a] β (base 10) is expressed as cm^{-1} of oxygen fluoride at S.T.P.

[b] $(v_1\nu_1 + v_2\nu_2 + v_3\nu_3) - \nu_{obs.}$

[c] Outside the range of the spectrograph, Hettner, et. al. gave 492 cm^{-1} for this band. Value given here was calculated from bands at 723 and 1240 cm^{-1}.

[d] Bands considered by Hettner, et. al. to be due to fluorocarbon impurities

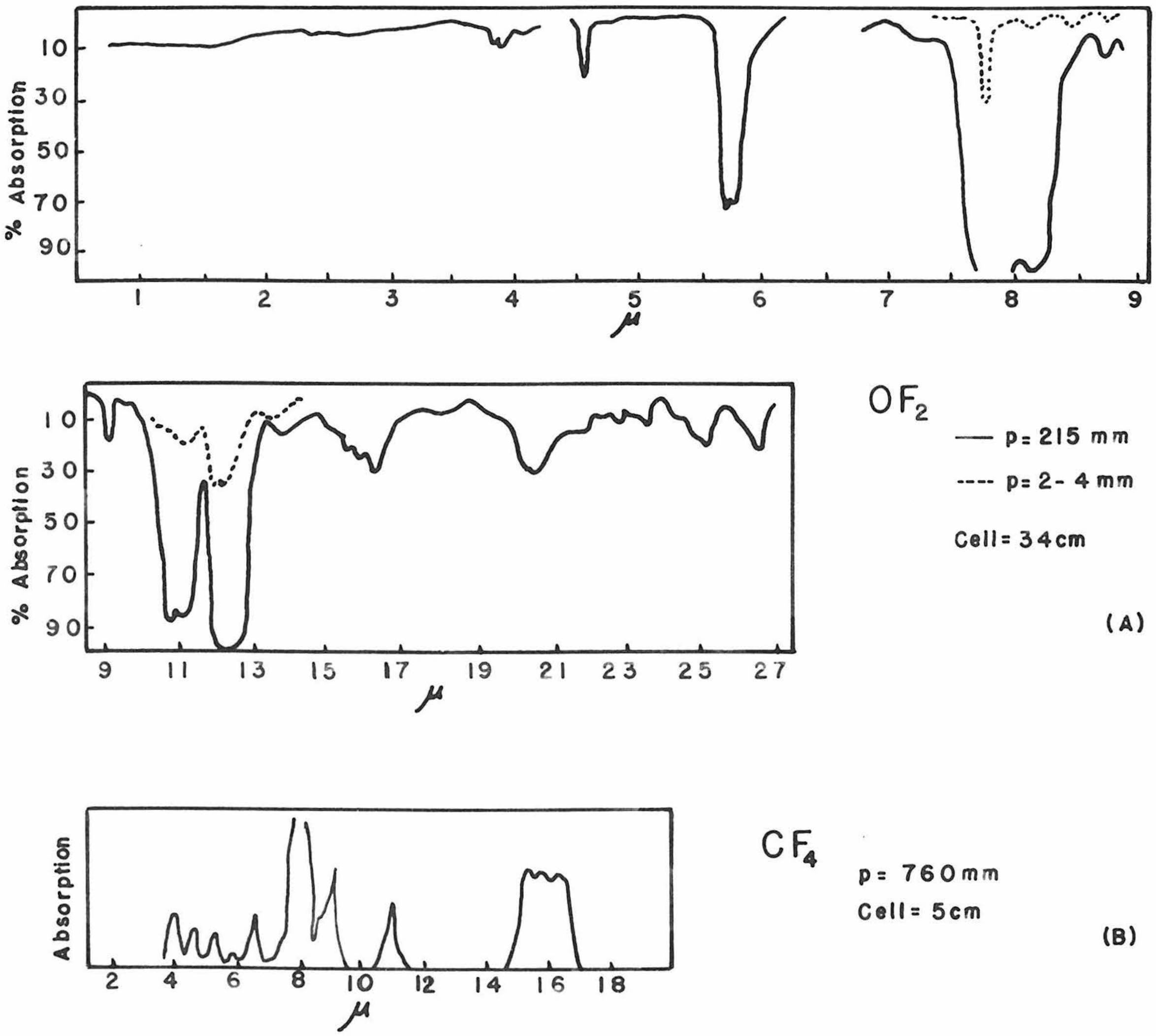

Figure 11. (A) The infrared absorption spectrum of oxygen fluoride as published by Hettner, Pohlmann, and Schumacher (37)

(B) The infrared absorption spectrum of carbon tetrafluoride as published by Bailey, Hale, and Thompson (40)

Bailey, Hale, and Thompson found at 630, 906, 1112, 2179, and 2541 cm^{-1}. Not only are the positions correct, but the relative intensities are closely similar.

Table 17

Carbon Tetrafluoride Bands Observed by Bailey, Hale, and Thompson (40)

ν (cm^{-1})
630
906
1112
1265
1360
1535
1696
1904
2179
2541

The bands observed at 723 and 1240 cm^{-1} in the present investigation were unreported by Hettner, et. al. However, these bands are present in their published spectra as the small peaks at 13.8 μ and 8.1 μ. We have assumed that the band at ~ 500 cm^{-1}, which we were unable to investigate because of the limitation of the sodium chloride prism, is due to oxygen fluoride and not to carbon tetrafluoride as the original investigators assumed. This assumption can be justified in several ways. The Raman spectrum of carbon tetrafluoride has been studied by Yost, Lassettre, and Gross (41) and only one line displaced by less than 630 cm^{-1} was found. This band at 437 cm^{-1} they ascribe to the doubly degenerate infrared inactive vibration ν_2. Also, the observed carbon fluoride bands can be satisfactorily explained without the assumption of a fundamental at ~500 cm^{-1}. The occurrence of the fundamental at 828 cm^{-1} and combination bands at 1282 and 1740 cm^{-1} plus the temperature sensitive band at 723 cm^{-1} necessitates the existence of a fundamental of oxygen fluoride at about 500 cm^{-1}. From the position of the difference band at 723 cm^{-1}, we assign a frequency of 517 cm^{-1} for the fundamental ν_2.

The present assignment of fundamentals is in agreement with the obtuse model as reported by electron diffraction studies and accounts satisfactorily for the observed band contours and intensities. However, the symmetric vibration, ν_1, is about 400 cm^{-1} higher in frequency than the asymmetric vibration, ν_3. In most other non-linear triatomic molecules ν_3 is higher or only slightly lower in frequency than ν_1. The contour of the band at 828 cm^{-1} cannot be mistaken; it clearly has a Q branch and is the most intense band in the oxygen fluoride spectrum. For an obtuse model this band must be the asymmetric valence vibration. If the 828 cm^{-1} band is to be the highest fundamental frequency, one of the other two fundamentals must have such a value as to yield the temperature sensitive band at 723 cm^{-1} as a difference band with 828 cm^{-1}. This would require a band at about 100 cm^{-1}. It appears extremely unlikely that oxygen fluoride would have a fundamental vibration at such a low frequency, since the lowest fundamental in ozone and in nitrogen dioxide is at 705 cm^{-1} and at 653 cm^{-1}, respectively.

Observed similarities in the spectra of nitrogen dioxide, ozone, and oxygen fluoride are discussed in Section E.

D. Some Observations on the Vibration Spectrum of Sulfur Dioxide

The correct vibrational assignment and molecular configuration of sulfur dioxide appears to be definitely established. The application of a simple valence-force normal coordinate treatment to the sulfur dioxide fundamentals yields an apex angle of 120° (42) which agrees well with the value of 121 ± 5° as found by electron diffraction (43). Because of this agreement between spectroscopic and electron diffraction data, it was of interest to compare the relative intensity of the sulfur dioxide bands with those of ozone, nitrogen dioxide, and oxygen fluoride. As discussed in Sections A and B, the spectroscopic data for ozone and nitrogen dioxide do not agree with the electron diffraction results. Further, it was of interest to determine if a band similar in character to the 1110 cm^{-1} band of ozone could be found on the high frequency side of ν_3 in sulfur dioxide. With an absorbing path of one meter at 25° C and sulfur dioxide pressure up to one atmosphere, no such band was observed. However, two previously unreported sulfur dioxide bands were observed at 2740 and 3620 cm^{-1}.

Tank sulfur dioxide (manufactured by Dow Chemical Co.) was used without further purification. The one-meter cell equipped with silver chloride windows was filled in the manner discussed in detail in Section B.

The infrared bands of sulfur dioxide are listed in Table 18 together with the band assignments and average apparent absorption

Table 18

Assignment and Approximate Apparent Absorption Coefficients for the Observed Sulfur Dioxide Bands

ν[a] (cm^{-1})	Assignment	β[b]	Band divergence[d]
(519)[c]	ν_2	-	
(606)[c]	$\nu_1 - \nu_2$	-	36
1151.2	ν_1	.32	
1361	ν_3	3.0	
1871	$\nu_2 + \nu_3$	.0015	9
2305	$2\nu_1$	.006	-2
2499	$\nu_1 + \nu_3$	.06	13
2740	$2\nu_1 + \nu_2$	.0009	82
3620	$2\nu_1 + \nu_3$	.002	44

[a] Except for the bands at 2740 and 3620 cm^{-1}, the frequencies given for the observed position are taken from Herzberg (42).

[b] β (base 10) expressed as cm^{-1} of sulfur dioxide at S.T.P.

[c] These bands could not be investigated with the spectrograph available.

[d] $(v_1\nu_1 + v_2\nu_2 + v_3\nu_3) - \nu_{obs}$.

coefficients. The assignment is that given by Herzberg (42). The apparent absorption coefficients represent the observed values of $(1/pL) \log_{10} T_0/T$ near the maximum of each band when the absorption is between fifteen and forty percent. Figure 12 is a plot of β versus frequency for sulfur dioxide. It is observed that ν_3 is considerably more intense than the symmetric valence vibration, ν_1, which is in agreement with observations made on other similar triatomic molecules.

The new bands observed at 2740 and 3620 cm^{-1} may be described as $2\nu_1 + \nu_2$ and $2\nu_1 + \nu_3$, respectively.

The region from 1.4 to 2.6 μ was scanned with the grating instrument described in Part II of this thesis, but with a path-length of 106 cm and a pressure of one atmosphere no bands were detected.

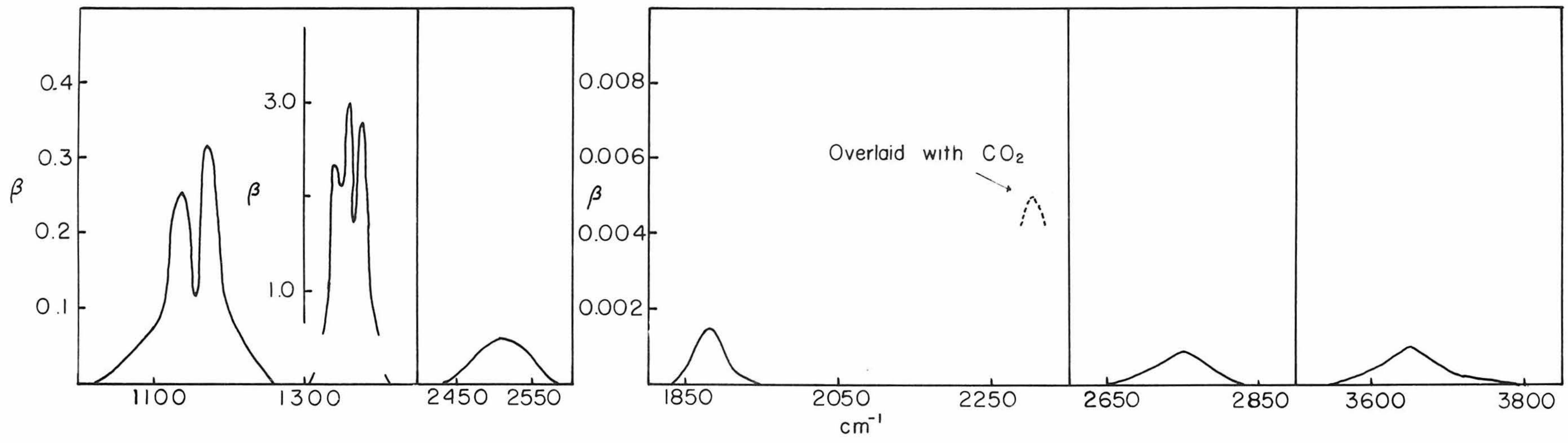

Figure 12. The observed infrared absorption spectrum of sulfur dioxide under low dispersion; $\beta = (1/pL) \log_{10} T_o/T$

E. Some Correlations between the Infrared Spectra and Structure of Several Triatomic Molecules

Non-linear, triatomic molecules for which the infrared spectrum and molecular structure are well understood have a relatively heavy atom in the apical position (e.g. water, hydrogen sulfide, sulfur dioxide), while ozone, nitrogen dioxide, and oxygen fluoride have apex atoms which are equal to or lighter in weight than the two atoms at the base of the isosceles triangle. It may be that each class of molecules can be discussed as a unit, but that correlations between the two groups may be rather obscure. In the following pages several observed regularities in the spectra and constitution of nitrogen dioxide, ozone, and oxygen fluoride are discussed, and some correlation with sulfur dioxide is attempted.

Various spectroscopic data for ozone, nitrogen dioxide, oxygen fluoride, and sulfur dioxide are collected in Table 19. The values given for the apical angles are those obtained by electron diffraction (6,19,34,43), and the values of the bond constant, K_1 , the bond-bond interaction constant, K_{12}, and the bending constant, K_{δ}/l^2, were calculated from the following relationships obtained from a modified valence-force normal coordinate treatment as reproduced by Herzberg:

$$\lambda_1 + \lambda_2 = \left(1 + \frac{2m_y}{m_x} \cos^2\alpha\right) \frac{K_1 + K_{12}}{m_y} + 2\left(1 + \frac{2m_y}{m_x} \sin^2\alpha\right) K_\delta / m_y l^2$$

$$\lambda_1 \lambda_2 = 2\left(1 + \frac{2m_y}{m_x}\right) \frac{K_1 + K_{12}}{m_y^2} \cdot \frac{K_\delta}{l^2}$$

$$\lambda_3 = \left(1 + \frac{2m_y}{m_x} \sin^2\alpha\right) \frac{K_1 - K_{12}}{m_y}$$

where $\lambda_i = 4\pi^2\omega_i^2$

ω_i = vibrational frequencies in 1/sec.

2α = apex angle

When considered in relation to sulfur dioxide, the low value of the bond constant for ozone seems remarkable. However, when compared with bond constants of more closely similar molecules, the value obtained for ozone does not appear to be unusual since the values of all three constants for ozone lie between those for nitrogen dioxide and oxygen fluoride. The values of K_1 and K_δ/l^2 decrease with decreasing apical angle and the interaction constant, K_{12}, increases.

Since the bond constant, K_1, decreases in this series, the value of ν_3 must also decrease for this frequency is determined primarily by K_1. It is observed that the value of ν_3 as well as the ratio of ν_3 to ν_1 decreases and is less than unity in both ozone and oxygen fluoride. This decrease in ν_3/ν_1 seems to be connected with the increase in the interaction constant, K_{12}. ~~That~~ ~~is, in the series, nitrogen dioxide - ozone - oxygen fluoride, the~~

Table 19

Comparison of the Vibration Spectrum and Force Constants for Several Triatomic Molecules

	Sulfur Dioxide		Nitrogen Dioxide		Ozone		Oxygen Fluoride	
	ν (cm^{-1})	β[a]	ν (cm^{-1})	β[a]	ν (cm^{-1})	β[a]	ν (cm^{-1})	β[a]
ν_2	519	-	648	-	705	0.07	517	-
$\nu_1 - \nu_2$	606	-					723	0.002
$\nu_3 - \nu_2$			833	0.04				
ν_1	1151.2	0.32	1306	.05	1110	.05	1240	.002
ν_3	1361	3.0	1615	2.5	1043	6.0	828	.17
$\nu_1 + \nu_2$			1910	.005			1740	.005
$\nu_1 + \nu_3$	2499	.06	2900	.15	2105	.15		
$\nu_2 + \nu_3$	1871	.0015			1740	.04	1282	.02
$2\nu_1$	2305	.006						
$2\nu_1 + \nu_2$	2740	.001						
$2\nu_1 + \nu_3$	3620	.002						
$\nu_1 + \nu_2 + \nu_3$			3545	.005	2800	.005		
$3\nu_3$			4760	.001	3050	.015		
$3\nu_3 + \nu_1$			5920	.0005				
2α	120°		132°		127°		100°	
I_{ν_3}/I_{ν_1}	10		50		120		100	
ν_3/ν_1	1.11		1.22		0.94		0.67	
K_1[b]	0.981×10^6		0.617×10^6		0.509×10^6		0.483×10^6	
K_{12}[b]	-0.019×10^6		-0.233×10^6		0.112×10^6		0.195×10^6	
K_δ/l^2	0.0877×10^6		0.261×10^6		0.148×10^6		0.087×10^6	

[a] $\beta = (1/pL) \log_{10} T_0/T$

[b] dynes/cm

~~presence of the second band on the apical atom appears to progressively weaken the first band.~~ This possible correlation between K_{12} and ν_3/ν_1 also may include sulfur dioxide, since the values of both K_{12} and ν_3/ν_1 for this compound lie between those for nitrogen dioxide and ozone. At the present time the proper quantitative relationship (if one exists) between the two quantities is not clear.

The observed spectra of nitrogen dioxide, ozone, and oxygen fluoride resemble each other with several exceptions. Difference bands are observed in nitrogen dioxide and oxygen fluoride, but not in ozone. This exception may be only apparent, since the difference bands which would be expected to occur in ozone with reasonable intensity fall beyond the region accessible with sodium chloride optics.

In nitrogen dioxide and ozone the combination band $\nu_1 + \nu_3$ occurs with considerable intensity. (The intensity as compared with ν_3 in nitrogen dioxide is 1 to 20, and 1 to 40 in ozone.) The corresponding band in oxygen fluoride was not observed with one meter of oxygen fluoride at atmospheric pressure. If this band possessed an intensity as great as one-eightieth that of ν_3 it would have been detected. Because of the low intensity of the oxygen fluoride fundamentals, the failure to observe the combination band $\nu_1 + \nu_3$ may be merely a result of the relatively weaker absorption in all bands.

There are a few additional non-linear triatomic molecules in which the apical atom is of smaller mass than the atoms at the base of the triangle, and which would exhibit fundamentals in the spectroscopically accessible region of the spectrum. The spectrum of chlorine monoxide was recorded under low dispersion some time ago (45). Nitrogen disulfide (46) and nitrosyl fluoride (47) are known but are difficult to work with and no spectra have been reported. An investigation of the vibration spectra of these molecules would provide additional data with which to test the suggestion made here that the value of ν_3 / ν_1 decreases as the apex angle of the molecule decreases. Also, it is of interest to determine the rotational structure of the perpendicular bands of chlorine monoxide and oxygen fluoride. If the rotational spacing is found to be in disagreement with that calculated for the molecular configuration as determined by electron diffraction, further evidence may be found to substantiate the existence of two overlapping bands in ν_2 of ozone and nitrogen dioxide.

Part II. The Infrared Spectrum and Configuration of Hydrogen Persulfide

Part II. The Infrared Spectrum and Configuration of Hydrogen Persulfide

1. Introduction

Although the structure of hydrogen peroxide has been the object of much experimental work and speculation (48), little attention has been paid to its sulfur analogue, hydrogen persulfide. The optimum conditions for maximum yield of hydrogen persulfide have been determined by Butler and Maass (49) who also studied a number of the physical properties of hydrogen persulfide. Stevenson and Beach (50) investigated the persulfide by means of electron diffraction and reported the S-S distance to be 2.05 ± .02 A. This definitely established that a single bond exists between the two sulfur atoms and infers that the hydrogens are bonded to separate sulfur atoms.

As a first approximation it is reasonable to assume that hydrogen persulfide would be similar in structure to hydrogen peroxide. From considerations of directed valence Penney and Sutherland (51) proposed a C_2 structure for hydrogen peroxide in which the O-O-H angle and the angle between the two O-O-H planes were about 100°. In the photographic infrared Zumwalt and Giguère (52) found two similar hybrid bands displaced 7.40 cm^{-1} from each other. These investigators considered this an example of inversion doubling and therefore a confirmation of the C_2 structure. No previous spectroscopic investigation has been reported on hydrogen persulfide.

The present work is concerned with an investigation of the vibration spectrum of hydrogen persulfide and the rotational structure of the symmetrical S-H stretching vibration at 2μ.

2. Experimental procedure and results

<u>Materials and methods</u> - The hydrogen persulfide used in this investigation was prepared by the procedure detailed by Butler and Maass (49). Briefly this method consists of dropping a sodium polysulfide solution (corresponding to about $Na_2S_{2.5}$) into cold, concentrated hydrochloric acid and fractionally distilling the hydrogen polysulfide formed. The colorless redistilled product was used immediately for the spectroscopic investigations. Two separate preparations were made and no spectroscopic difference was noted.

To keep decomposition of the hydrogen persulfide at a minimum the absorption cells were cleaned with boiling concentrated nitric acid. The cells were dried thoroughly and then acidified with hydrogen chloride gas. The hydrogen chloride gas was allowed to remain in the cell for 10-15 minutes before the cell was evacuated and the hydrogen persulfide introduced. Since hydrogen persulfide is a liquid at room temperature, the evacuated cell was filled at a known pressure by immersing the trap containing the liquid hydrogen persulfide in a bath of known temperature and allowing the stopcock between the cell and the trap to remain open while the spectrum was traced.

An attempt to use silver chloride windows made vacuum tight with Koroseal gaskets was unsuccessful. The persulfide decomposed very rapidly on the silver chloride surface to yield an opaque deposit of sulfur. When sodium chloride windows were substituted only slight decomposition occurred over a period of two hours.

The vibration spectrum was traced from 1.5 to 15 μ with the Beckman IR-2 spectrophotometer described in Part I, Section A, of this thesis. A 50-cm cell was employed and traces were taken with the trap at 0° (v.p. 33 mm), and at 25° C (v.p. 109 mm). The bands observed, the approximate apparent absorption coefficients, and proposed assignment are listed in Table 20. Figure 13 contains a reproduction of the hydrogen persulfide spectrum.

Table 20

Assignment and Approximate Apparent Absorption Coefficients for the Observed Hydrogen Persulfide Bands

ν (cm^{-1})	β^{a}	Assignment	(cm^{-1})
(530)[c]	-	ν_3	-
$886\begin{cases}875\\897\end{cases}$	0.035 .043	ν_6 or $\begin{cases}\nu_4\\\nu_6\end{cases}$	-
2577	.015	ν_1, ν_2	-
3065	.002	$\nu_3 + (\nu_2, \nu_1)$	42[c]
3400	.002	$(\nu_6, \nu_4) + \nu_2$	74,52
5007.2	.003	$2\nu_1$	147

[a] β (base 10) cm^{-1} pure hydrogen persulfide at S.T.P.

[b] $(v_1\nu_1 + v_2\nu_2 + \cdots) - \nu_{\text{obs.}}$

[c] See text

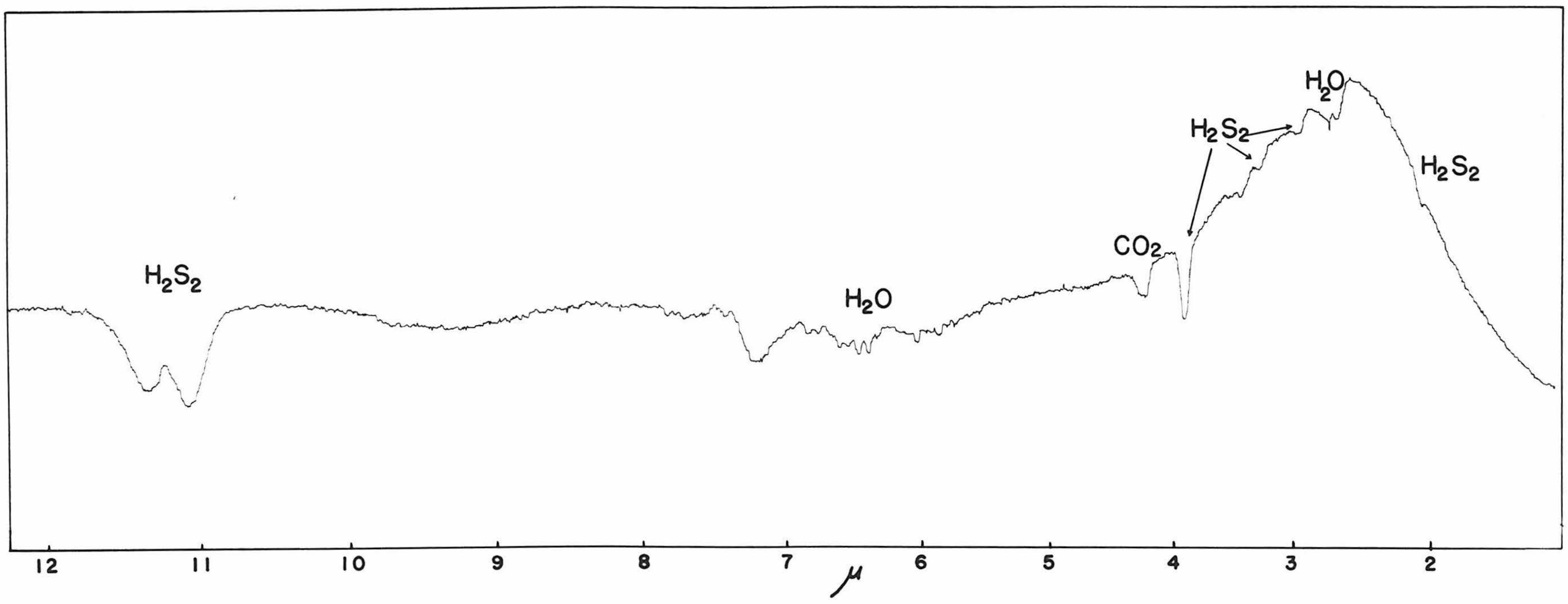

Figure 13. The observed hydrogen persulfide bands at 25° C; equivalent pathlength = 6.2 cm

Grating instrument - The 2μ band was also investigated under high dispersion. The instrument used was an automatic recording one-meter vacuum spectrograph with a lead sulfide cell as the photosensitive element. This instrument has been described recently (53) by Badger, Zumwalt, and Giguère. The spectra were taken in the first order of a 7500 line per inch replica grating cast from an original ruled by Wood. A slit width of 0.05 mm corresponding to 0.85 cm^{-1} was used in this region.

The instrument was calibrated by observing first and higher orders of visible and near-infrared argon lines from a sodium vapor lamp containing argon at low pressure. A plot of λ_{vac}/N against λ_{vac} was then constructed where N, recorded by a Veeder counter, is directly proportional to the rotation of the lead screw. The counter read zero when the grating was perpendicular to the light beam. Every ten turns of the counter was recorded on the trace by a "pip". The counter number corresponding to each absorption line in the spectrum was then determined by linear interpolation between the wavelength markers. The value of λ_{vac}/N corresponding to the approximate wavelength of the line was read from the calibration chart, and the wavelength for each line calculated. All calculations were performed with a Monroe automatic calculator. The wavelength measurements are believed accurate to 1 part in 25000. The frequencies listed in Table 21 are the average of measurements on two different traces of the 2.0μ hydrogen persulfide band. A tracing of this band is reproduced in Figure 14.

Table 21

Positions of the Sub-bands in the Hydrogen Persulfide Band at 2 μ

Assignment	ν_{vac}[a] (cm^{-1})	$\Delta\nu$[b]	Assignment	ν_{vac}[a] (cm^{-1})	$\Delta\nu$[b]
^{R}Q	5099.4*		^{R}Q	5012.0*	
	96.5	6.4		05.0	9.7
^{R}Q	93.0*		^{P}Q	02.3*	
	89.6	5.9		4999.8	
^{R}Q	87.1*	6.0		97.8	9.5
^{R}Q	81.1*			95.0	
	78.7	6.5	^{P}Q	92.8*	
^{R}Q	74.6*	7.3		88.5	9.6
^{R}Q	67.3*		^{P}Q	83.2*	
	65.1	7.0		78.9	9.8
^{R}Q	60.3*		^{P}Q	73.4*	
	58.0	7.4		68.4	10.0
	56.1		^{P}Q	63.4*	
^{R}Q	52.9*			58.5	10.6
	50.0	7.3	^{P}Q	52.8*	
^{R}Q	45.6*	8.0		48.6	11.0
^{R}Q	37.6*		^{P}Q	41.8*	11.7
	34.4	8.1	^{P}Q	30.1*	
^{R}Q	29.5*			25.4	11.4
	24.5	8.5	^{P}Q	18.7*	11.9
^{R}Q	21.0*		^{P}Q	06.8*	10.6
	17.2	9.0	^{P}Q	4896.2*	

[a] The intense "lines" are marked with an asterisk.

[b] Between intense "lines"

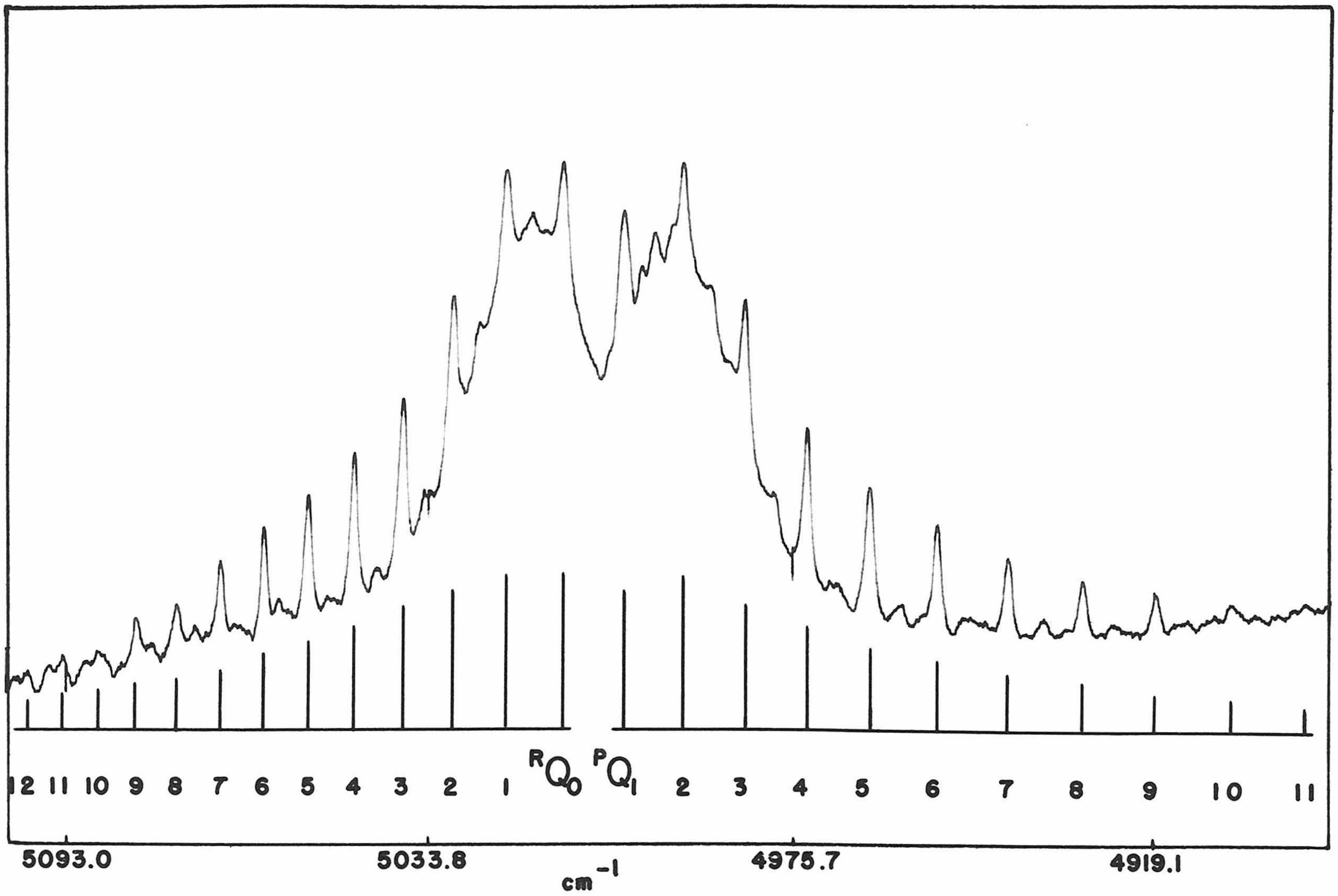

Figure 14. Rotational structure of the hydrogen persulfide band $2\nu_1$; equivalent pathlength = 12.4 cm

Possible contamination by hydrogen sulfide - A hydrogen sulfide band is known to be at 1.9μ. It was conceivable that enough hydrogen sulfide would be formed by decomposition of the persulfide during the tracing to interfere with the spectrum of the 2.0μ persulfide band; therefore, the spectrum of hydrogen sulfide was investigated from 1.3 to 2.5μ in the grating instrument. Tank hydrogen sulfide (manufactured by Ohio Chemical and Manufacturing Co.) was condensed in a trap surrounded by a dry ice - methanol mixture. Phosphorous pentoxide had previously been introduced into the trap. A second trap containing phosphorous pentoxide was then cooled in dry ice - methanol and the first trap allowed to warm up to $\sim -40^\circ$ C. The condensate in the second trap was used immediately for the spectroscopic investigation. The hydrogen sulfide spectrum was taken in a 106-cm cell with pyrex windows with the gas at a pressure of one atmosphere. Two bands of hydrogen sulfide were found: the band known to be at 1.9μ, and a previously unreported band at 1.6μ. Both bands exhibit collected Q branches and, therefore, are parallel bands. No analysis has yet been attempted for these bands. The frequencies of the rotational maxima observed are given in Tables 22 and 23. The running numbers assigned to the lines are for identification purposes only and have no other significance. Traces of the 1.9 and 1.6μ bands are reproduced in Figures 15 and 16, respectively.

Table 22

Positions of the Observed Rotational Lines in the 1.9 μ Band of Hydrogen Sulfide

No.	ν (cm^{-1})	No.	ν (cm^{-1})	No.	ν (cm^{-1})
1	5268.8	34	5174.2	68	5081.0
2	63.6	35	70.1	69	78.6
3	60.0	36	66.3	70	75.1
4	57.3	37	63.8	71	73.0
5	55.3	38	60.0	72	70.7
6	51.6	39	58.0	73	69.7
7	49.6	40	54.4	74	67.1
8	45.9	41	50.2	75	65.7
9	43.9	42	48.4	76	63.2
10	40.7	43	45.1	77	60.0
11	37.7	44	41.7	78	58.2
12	33.8	45	38.4	79	55.6
13	31.2	46	37.3	80	50.8
14	28.0	47	34.2	81	46.6
15	24.3	48	32.5	82	44.2
16	21.6	49	30.0	83	41.3
17	18.9	50	28.5	84	36.8
18	17.0	51	25.9	85	35.0
19	14.0	52	23.0	86	32.6
20	10.0	53	19.6	87	27.7
21	07.0	54	17.2	88	23.3
22	03.9	55	14.9	89	21.3
23	02.4	56	12.7	90	16.5
24	00.1	57	10.2	91	11.0
25	5198.1	58	08.0	92	07.6
26	94.5	59	03.6	93	04.1
27	92.3	60	02.5	94	4995.8
28	86.3	61	00.6	95	92.4
29	85.3	62	5099.0	96	88.5
30	82.5	63	96.6	97	85.4
31	81.2	64	92.1	98	80.4
32	78.3	65	89.6	99	72.0
33	76.9	66	87.9	100	64.2
		67	85.0		

Table 23

Positions of the Observed Rotational Lines in the 1.6 μ Band of Hydrogen Sulfide

No.	ν (cm^{-1})	No.	ν (cm^{-1})	No.	ν (cm^{-1})
1	6428.9	28	6332.3	56	6245.7
2	25.0	29	28.7	57	41.1
3	18.0	30	23.6	58	36.7
4	15.7	31	20.2	59	35.3
5	11.4	32	15.1	60	31.6
6	08.1	33	12.4	61	25.8
7	06.1	34	09.2	62	23.2
8	02.6	35	05.9	63	17.1
9	6399.6	36	02.3	64	14.6
10	97.7	37	01.1	65	11.3
11	93.4	38	6296.3	66	06.6
12	88.4	39	91.5	67	03.4
13	85.2	40	89.2	68	6199.2
14	81.7	41	87.5	69	94.8
15	79.3	42	85.6	70	91.5
16	75.2	43	81.8	71	89.7
17	70.1	44	77.4	72	87.0
18	67.7	45	75.6	73	83.9
19	63.6	46	73.1	74	79.8
20	58.0	47	71.7	75	74.9
21	56.1	48	67.7	76	68.4
22	54.6	49	66.2	77	64.7
23	51.3	50	64.7	78	61.8
24	48.3	51	62.2	79	55.8
25	44.5	52	57.8	80	48.9
26	40.8	53	55.5	81	44.0
27	36.5	54	52.5	82	29.7
		55	48.6		

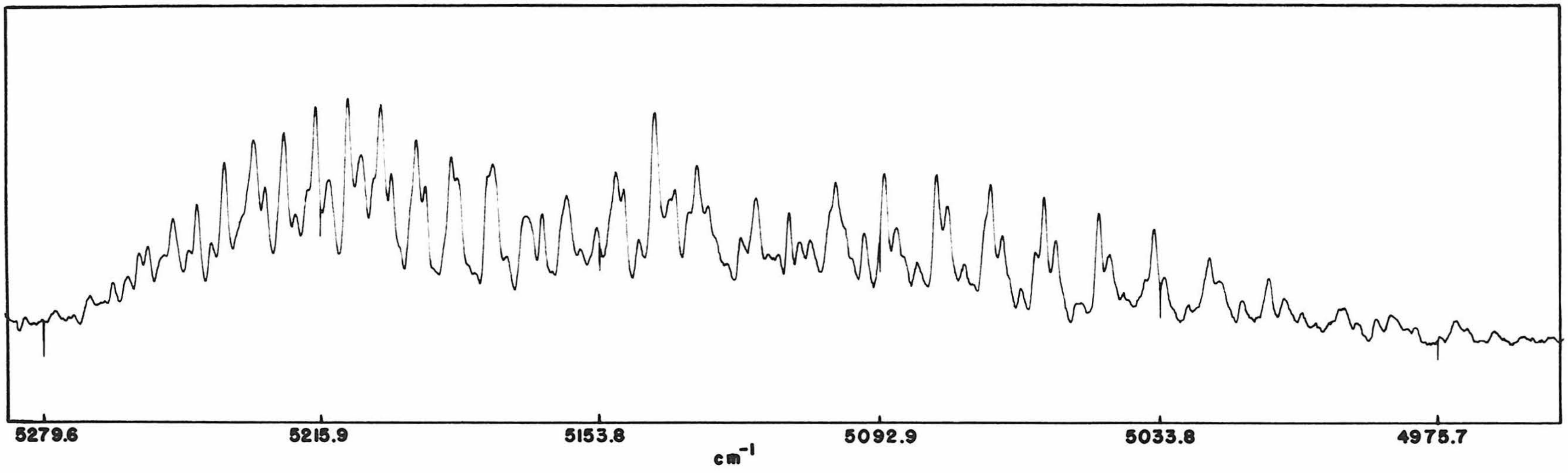

Figure 15. Rotational structure of the 1.9 μ band of hydrogen sulfide; equivalent pathlength = 96 cm

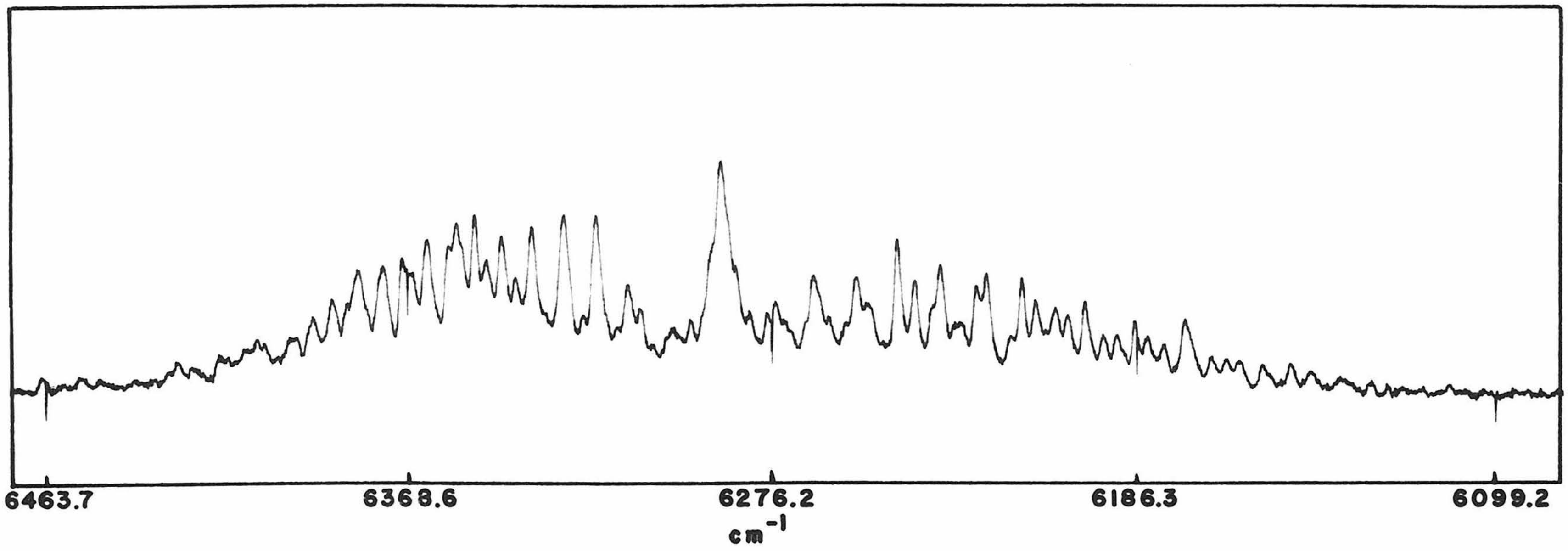

Figure 16. Rotational structure of the 1.6 μ band of hydrogen sulfide; equivalent pathlength ≈ 96 cm

Although the hydrogen sulfide and hydrogen persulfide bands occur in the same region of the spectrum, no contamination of the hydrogen persulfide band at 2 μ was evident under the conditions employed.

3. Discussion

(a) Vibrational analysis

The S-S distance of 2.05 ± .02 A, as determined by Stevenson and Beach (50), agrees very well with the single-bond distance for sulfur (2.08 A), as calculated from the radii given by Pauling (54). It then seems certain that the S-S bond in hydrogen persulfide is single. This conclusion is substantiated by the electron diffraction studies of sulfur monochloride (55,56) and dimethyl disulfide (50) in which the S-S bond was found to be single. Since hydrogen sulfide and the two disulfide compounds above are known to be non-linear, it is reasonable to assume the S-S-H angle in hydrogen persulfide to be somewhere between 93°, as observed in hydrogen sulfide, and 107° or 103°, as observed in dimethyl disulfide and sulfur monochloride, respectively. Thus, we have assumed a C_2 structure for the hydrogen persulfide molecule.

The six fundamental vibrations of hydrogen persulfide may be described as two S-H valence vibrations, two S-S-H bending vibrations, a torsional oscillation, and a vibration in which the two S-H groups vibrate against each other. The observed infrared bands of hydrogen persulfide are listed in Table 20 together with a proposed assignment on the basis of the assumed C_2 structure. The values given in Column 2 for each band represent the average value of $(1/pL) \log_{10} T_0/T$ near the maximum of each band when the absorption is between 15 and 50 percent. The band at 2577 cm^{-1} can be identified as an S-H stretching frequency from its proximity to the asymmetric S-H frequency in hydrogen sulfide which is located at 2684 cm^{-1} (57). Only one band was observed in this region for hydrogen persulfide which agrees with the observation of only one O-H valence frequency in hydrogen peroxide (58). The identity of the maxima at 875 and 897 cm^{-1} is not obvious. Although the S-H bending vibrations would be assumed to lie in this region, the symmetric vibration, ν_4, would be expected to be weak. From intensity considerations it seems likely that the two maxima represent the P and R branches of the asymmetric bending frequency, ν_6. Since this vibration produces a changing dipole moment parallel to the top axis, it would possess a Q branch in addition to P and R branches. That a Q branch is not observed may mean only that it is ill-defined and therefore not prominent under low dispersion. The possibility must also be considered that these two maxima represent two unresolved bands. The S-S vibration, which would be very weak in the infrared, in all probability lies outside the range of the Beckman instrument; however, it is possible to approximate its position. The value given in Table 20 for this frequency was approximated in the following manner. The frequency of this vibration may be expected to lie considerably lower than the S-S frequency in diatomic sulfur, 725.8 cm^{-1} (59), but higher than that in S_8 , 474 cm^{-1} (60), or than in sulfur monochloride, 445 cm^{-1} (61). The hydrogen persulfide band at 3065 cm^{-1} may be described as a combination of this S-S vibration with the S-H vibration at 2577 cm^{-1}. Assuming a reasonable anharmonicity constant, a value of about 530 cm^{-1} is obtained for ν_3. This value must be considered only approximate until the Raman spectrum of hydrogen persulfide has been investigated. At present no estimate can be made of the torsional vibration, ν_5.

(b) Rotational analysis of 2 μ band

<u>Assignment of 2 μ band</u> - Figure 14 is a reproduction of the high dispersion tracing of the 2 μ band of hydrogen persulfide. This band closely resembles a perpendicular band of a symmetric top. The ^PQ and ^RQ branches are approximately evenly spaced and, although there is a slight minimum in intensity in the middle of the band, no ^PQ or ^RQ branches are missing. This band almost certainly should be given one of the three following assignments: $2\nu_1$, $2\nu_2$, or $\nu_1+\nu_2$, where ν_1 is the symmetric S-H vibration and ν_2 is the asymmetric vibration. Assuming hydrogen persulfide to be nearly a prolate top, the axis of least moment of inertia is the top axis. The symmetric vibration produces a changing dipole moment nearly perpendicular to the least axis and therefore is a near-perpendicular type band which would exhibit a single maximum with ^PQ and ^RQ branches about evenly spaced. In the asymmetric vibration the changing dipole is almost in the direction of the top axis and the

band would contain a collected Q branch in addition to P and R branches. Symmetry considerations for the C_2 model show that both $2\nu_1$ and $2\nu_2$ would be essentially perpendicular bands while $\nu_1 + \nu_2$ would closely resemble a parallel band. It is generally found that the even harmonics of similar asymmetric vibrations (ν_3 in water, for example) are extremely weak or are missing altogether. Thus, it can be considered most probable that the hydrogen persulfide band at 2 μ is the first overtone of the symmetric S-H valence vibration, ν_1 .

<u>Observed least moment of inertia</u> - Table 21 contains the wave numbers of the sub-bands observed in the 2 μ band as well as their assignment and the separation of the most intense sub-bands.

The rotational energy of a near-prolate symmetric top may be represented by:

$$F_{(v)}\ (J,K) = \tfrac{1}{2}(B_{(v)} + C_{(v)})J(J+1) + (A_{(v)} - \tfrac{1}{2}(B_{(v)} + C_{(v)}))K^2$$

$$\text{where } A_{(v)} \gg B_{(v)} \approx C_{(v)}$$

The subscripts on the rotational constants indicate the average values of the constants during a vibration, which differ in general from the equilibrium values, A_e, B_e, and C_e. The equilibrium values are defined as:

$$A_e = \frac{h}{8\pi^2 c I_{A_e}} \quad ; \quad B_e = \frac{h}{8\pi^2 c I_{B_e}} \quad ; \quad C_e = \frac{h}{8\pi^2 c I_{C_e}}$$

Here I_{A_e}, I_{B_e}, and I_{C_e} are the equilibrium values of the moment of inertia around the axis of least, intermediate, and greatest moment of inertia, respectively.

From an analysis of a perpendicular band of a nearly prolate symmetric top, accurate values of $(A_{(v)} - \frac{1}{2}(B_{(v)} + C_{(v)}))$ in both the upper and lower states may be obtained from the combination differences (62)

$$
\begin{aligned}
{}^{R}Q_{K-1} - {}^{P}Q_{K+1} &= \Delta_2{}^{K}F''(J,K) = F''(J,K+1) - F''(J,K-1) \\
&= 4(A''_{(v)} - \tfrac{1}{2}(B''_{(v)} + C''_{(v)}))K
\end{aligned}
$$

and

$$
\begin{aligned}
{}^{R}Q_{K} - {}^{P}Q_{K} &= \Delta_2{}^{K}F'(J,K) = F'(J,K+1) - F'(J,K-1) \\
&= 4(A'_{(v)} - \tfrac{1}{2}(B'_{(v)} + C'_{(v)}))K
\end{aligned}
$$

The values of $(A_{(v)} - \frac{1}{2}(B_{(v)} + C_{(v)}))$ for both the upper and lower state obtained in this manner are tabulated in Table 24.

Table 24

Combination Differences for Upper and Lower States of the 2 μ Band of Hydrogen Persulfide

K	${}^RQ_{K-1} - {}^PQ_{K+1}$ (cm^{-1})	$(A''_{(v)} - \frac{1}{2}(B''_{(v)} + C''_{(v)}))$ (cm^{-1})	${}^RQ_K - {}^PQ_K$ (cm^{-1})	$(A'_{(v)} - \frac{1}{2}(B'_{(v)} + C'_{(v)}))$ (cm^{-1})
1	19.2	4.80	18.7	4.67
2	37.8	4.73	36.7	4.59
3	56.1	4.60	54.4	4.53
4	74.2	4.64	72.2	4.51
5	92.8	4.64	89.5	4.48
6	111.1	4.63	107.5	4.48
7	130.2	4.65	125.5	4.48
8	148.6	4.64	144.5	4.51
9	167.8	4.66	162.4	4.51
10	184.9	4.62	180.3	4.51
11			196.8	4.47

Calculation of principle moments of inertia - The configuration of the persulfide molecule may be considered to be a function of four parameters: the S-S distance, S-H distance, S-S-H angle, and the angle between the two S-S-H planes. The S-H distance is in all probability equal to that found in hydrogen sulfide, 1.334 A (63). Assuming this value for the S-H distance and knowing the three moments of inertia, the configuration of the molecule could be determined. Since only the value of $(A_{(v)}-\frac{1}{2}(B_{(v)}+C_{(v)}))$ was determined in the present investigation, the configuration can only be approximated. The probable extreme values for the S-H distance, S-S distance, and the S-S-H angle can be obtained from spectroscopic and electron diffraction data on similar molecules. By calculating the three moments of inertia with the extreme values of the above three parameters and various values of the angle between the two S-S-H planes, the values of this angle compatible with the observed value of $(A_{(v)}-\frac{1}{2}(B_{(v)}+C_{(v)}))$ can be determined.

To make these calculations it is necessary to derive general expressions for the three principal moments of inertia for the C_2 model of hydrogen persulfide. Consider the following three projections of the hydrogen persulfide molecule.

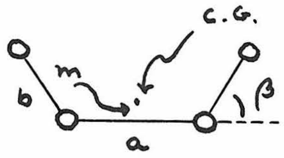

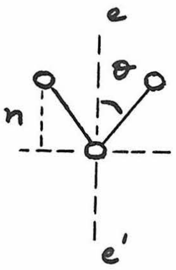

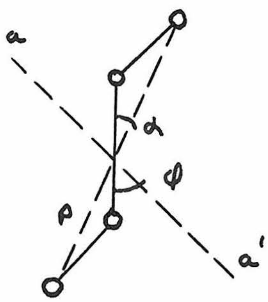

where β is the angle between the extension of the S-S bond and the S-H bond, θ is one-half the angle between the two S-S-H planes, a is the S-S distance, and b is the S-H distance.

It is desired to find the moment of inertia about any axis through the center of gravity and in a plane perpendicular to the e-e' plane. The angle this axis makes with the e-e' plane is designated as ϕ. By minimizing this moment of inertia with respect to ϕ, the axis of least moment of inertia (I_A) of the molecule will be defined. I_B and I_C will then be the moments of inertia around an axis at right angles to both the a-a' axis and to the e-e' plane, and the C_2 axis, respectively.

The three principal moments of inertia are found to be (see Appendix):

$$I_A = 2\left[(n-m)^2 + p^2 \mathrm{Sin}^2(\phi+\alpha)\right] + 64\left[m^2 + a^2/4\ \mathrm{Sin}^2\phi\right]$$

$$I_B = 2\left[(n-m)^2 + p^2 \mathrm{Sin}^2\left[90-(\phi+\alpha)\right]\right] + 64\left[m^2 + a^2/4\ \mathrm{Sin}^2(90-\phi)\right]$$

$$I_C = 2\left[p^2\right] + 64\left[a^2/4\right]$$

where $n = b\ \mathrm{Sin}\,\beta\ \mathrm{Cos}\,\theta$

$m = b/32\ \mathrm{Sin}\,\beta\ \mathrm{Cos}\,\theta$

$p^2 = (b\ \mathrm{Cos}\,\beta + a/2)^2 + (b\ \mathrm{Sin}\,\beta\,\mathrm{Sin}\,\theta)^2$

$\alpha = \mathrm{Tan}^{-1}\ (b\ \mathrm{Sin}\,\beta\ \mathrm{Sin}\,\theta)/(b\ \mathrm{Cos}\,\beta + a/2)$

$\mathrm{Sin}\ 2\phi = (p^2\,\mathrm{Sin}\ 2\alpha)/(p^4 + 64a^4 + 16a^2p^2\,\mathrm{Cos}\ 2\alpha)^{1/2}$

The least moment of inertia, I_A, is a function of four variables: a, b, θ, β. The S-H distance, b, is taken as equal to the distance observed in hydrogen sulfide, 1.33 ± .00 A (63). The S-S distance as determined by electron diffraction (50) is 2.05 ± .02 A. The H-S-H angle in hydrogen sulfide is 93° (63), the S-S-Cl angle in sulfur monochloride is 103°, and the S-S-C angle in dimethyl disulfide is 107°. Since β is 180° minus the included angle, it seems reasonable to let β range from about 75° to 85°. The problem is, then, to determine what value of θ when combined with the extreme values of the other variables will yield values of $A_{(v)} - \frac{1}{2}(B_{(v)} + C_{(v)})$ in agreement with that observed. An increase in a, b, or β increases I_A and, therefore, decreases A. Thus, the calculated value of θ will have its minimum value in agreement with observation when a, b, and β are largest, and its maximum value when a, b, and β have their minimum value. When $a = 2.07$ A, $b = 1.33$ A, and $\beta = 85°$, it is found that the calculated value of $A_{(v)} - \frac{1}{2}(B_{(v)} + C_{(v)})$ is too low for all values of θ greater than ~10° and too high for values of θ less than 10°. For $a = 2.03$ A, $b = 1.33$ A, and $\beta = 75°$, the calculated value is too high for values of θ smaller than about 37° and too low for values of θ greater than 37°. Representative values of $A - \frac{1}{2}(B + C)$ calculated for various values of a, b, θ, and β are listed in Table 25.

Table 25

Values of the Rotational Constants Calculated for Various Bond Distances and Bond Angles for Hydrogen Persulfide

θ (deg)	β (deg)	a (A)	b (A)	A (cm^{-1})	B (cm^{-1})	C (cm^{-1})	$A-\frac{1}{2}(B+C)$* (cm^{-1})
0	85	2.07	1.33	4.95	0.23	0.24	4.71
5	85	2.07	1.33	4.92	.23	.24	4.68
10	85	2.07	1.33	4.87	.23	.24	4.64
15	85	2.07	1.33	4.84	.23	.24	4.60
90	85	2.07	1.33	4.56	.25	.22	4.32
0	75	2.03	1.33	5.23	0.23	0.24	5.00
30	75	2.03	1.33	5.05	.23	.24	4.81
35	75	2.03	1.33	4.92	.24	.23	4.68
40	75	2.03	1.33	4.83	.24	.23	4.59
45	75	2.03	1.33	4.77	.24	.23	4.53
90	75	2.03	1.33	4.43	.24	.23	4.20

* observed value = 4.64 cm^{-1}

Since in the present investigation only a perpendicular band could be investigated under high resolution, effectively only the small moment of inertia of the hydrogen persulfide molecule is known with accuracy. Depending on the values assigned the other angle and the two distances, the angle between the two S-S-H planes may assume any value between 10° and 75°.

Comparison with hydrogen peroxide - The difference in appearance between the first overtone of ν_1 in hydrogen peroxide and the corresponding S-H band in hydrogen persulfide is striking. The $2\nu_1$ band in peroxide is identical in appearance to the photographic band investigated by Zumwalt and Giguère (52). These two bands are of the hybrid type showing both perpendicular and parallel character, and each band appears to consist of two identical bands separated by only a few wave numbers. The peroxide band, $2\nu_1$, has an unmistakable Q branch and the ^PQ and ^RQ branches of the perpendicular part are not at all prominent. In the $2\nu_1$ band of hydrogen persulfide the ^PQ and ^RQ branches are very prominent and no suggestion of a collected Q branch is observed. The appearance of a hybrid band indicates that the changing dipole moment is not at 90° with the top axis. This enabled Zumwalt and Giguère to rule out the cis configuration for hydrogen peroxide. Since the corresponding persulfide band shows no detectable hybrid character, it is not possible to eliminate a near-cis configuration for hydrogen persulfide. Thus, the azimuthal angle in hydrogen persulfide may be considerably smaller than that in hydrogen peroxide.

Part III. Some Observations on the Spectrum of "Sulfur Monoxide"

Part III. Some Observations on the Spectrum of "Sulfur Monoxide"

1. Introduction

Sulfur monoxide has been postulated as an intermediate in the production of sulfur-oxygen compounds such as the polythionates. In an attempt to find a method to produce significant amounts of sulfur monoxide, Schenk passed a mixture of sulfur dioxide and sulfur vapor through a glow discharge. After the gas had passed through the discharge tube, it exhibited a characteristic absorption spectrum between 2500 and 3400 A which was attributed to the presence of SO, sulfur monoxide (64). The absorption was very strong and completely masked the sulfur dioxide bands, although the new absorbing material, according to Schenk, amounted to only about one percent of the total gas. During the next ten years Schenk and various collaborators conducted numerous investigations concerning the methods of preparation and properties of this material which had been identified as sulfur monoxide (65).

Schenk and his co-workers found that the material could be produced by passing sulfur dioxide alone or sulfur dioxide and sulfur vapor through a discharge, but the most satisfactory method from the standpoint of yield was to burn sulfur in oxygen at a pressure of 10 mm. This method reportedly gave a 40-percent yield of the new substance.

The identity of the material which Schenk has termed "sulfur monoxide" is by no means settled. Cordes, although apparently originally in agreement with Schenk (65), some years later published a paper (66) in which he concluded that the absorption spectrum in question was due to a metastable S_2^* molecule and not to sulfur monoxide.

Several Russian investigators, Yakovleva, V. Kondrat'eva, and E. Kondrat'eva (67,68,69), have worked with Schenk's "sulfur monoxide" and have concluded that the carrier of the absorption spectrum is S_2O_2.

The present investigation was undertaken with the hope that sufficient amounts of the new substance could be obtained to allow the unique determination of its molecular structure. Unfortunately, this end was not achieved, but experiments were performed which yielded additional information concerning the identity of this sulfur compound.

2. Experimental procedure and results

(a) Search for the "Schenk Bands" under conditions which yield the SO emission spectrum

SO emission spectrum - The "Schenk Bands" are observed in absorption at room temperature and, therefore, must involve the ground state or a metastable excited state of the molecule. An emission spectrum known to be due to SO occurs in an electric discharge through sulfur dioxide, and Martin (70) has concluded that the lower state in the emission spectrum of SO is the ground state. Thus, if, as Schenk contends, SO is the carrier of this absorption spectrum, it is reasonable to assume that the "Schenk Bands" would occur under conditions which were favorable for the production of the SO emission spectrum.

In addition to Martin's analysis of the SO emission bands there is another test which may be applied to indicate whether the ground state of SO has been correctly determined. Badger's Rule (71) gives a relation between the bond force constant and the internuclear distance. If the ground states have been correctly determined for the series O_2, SO, and S_2, a straight line should be obtained from a plot of the internuclear distance against the reciprocal of the cube root of the force constant. The values of K and r_e contained in Table 26 were taken from Herzberg (59). It is seen in Figure 17 that a plot in the manner indicated does yield a straight line. It now appears reasonably conclusive that the ground state of the SO molecule is involved in the observed emission spectrum.

Table 26

Some Molecular Constants for O_2, SO, and S_2

	r_e[a] (A)	ω_e (cm^{-1})	μ_A (g)	K[b] (dynes/cm)	$K^{1/3}$	$K^{-1/3}$
O_2	1.2076	1580.36	8.000	1.177×10^6	105.5	0.0095
SO	1.4935	1123.73	10.67	7.938×10^5	92.60	.0108
S_2	1.89	725.8	16.00	4.964×10^5	79.18	.0126

[a] Values of r_e and ω_e are taken from Herzberg (59).

[b] $K = 5.8894 \times 10^{-2} \mu_A \omega_e^2$

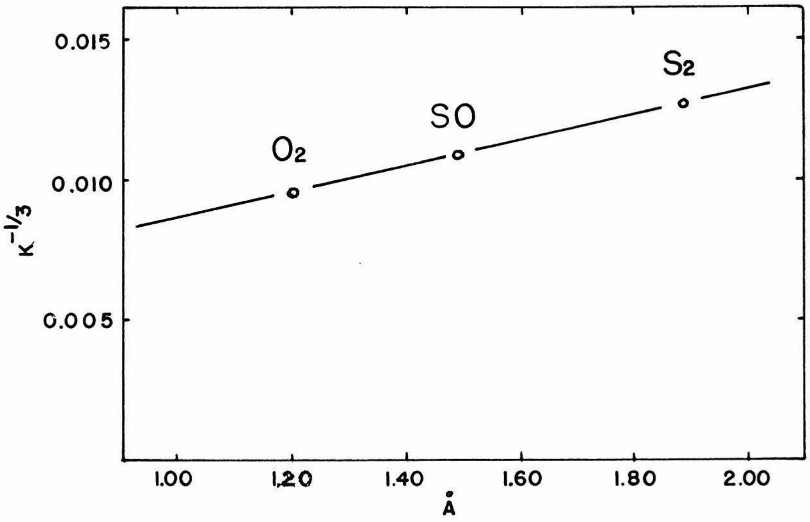

Figure 17. Relationship between $K^{-1/3}$ and r_e in the series: oxygen, sulfur monoxide, sulfur

The concentration of SO molecules should be greatest during or immediately after the discharge through sulfur dioxide. Therefore, if the spectrum reported by Schenk is due to the presence of SO molecules, the absorption should be most intense under the conditions which yield a strong emission spectrum of SO.

The system was arranged to permit the absorption spectrum of the gas in the discharge tube to be obtained during the periods when the discharge tube was dark. Since the discharge through the sulfur dioxide flashed at the rate of 120 times a second, the absorption spectrum was obtained within 1/120 of a second after the SO emission spectrum was produced.

Hydrogen-discharge tube - A hydrogen-discharge tube operating on a continuous flow of hydrogen at low pressure was employed as a source of continuous radiation. Although a discharge through hydrogen produces a usable continuum from about 3500 to 1200 A, the presence of small amounts of oxygen is detrimental due to the OH emission bands at 3060 A. Consequently, it was necessary to remove traces of oxygen found in commercial tank hydrogen prior to use in the discharge tube. The purifying train illustrated in Figure 18 consists, in the order named, of a differential manometer, hot platinum wire, drying column of Desichlora and Indicating Drierite, a low-pressure leak, and a low-pressure manometer. The hydrogen pressure was reduced from slightly above atmospheric pressure to about 2 mm by pumping on an unglazed porcelain leak (Stupakoff tubing) with a HyVac oil pump. The rate of flow of the hydrogen through the porcelain was adjusted

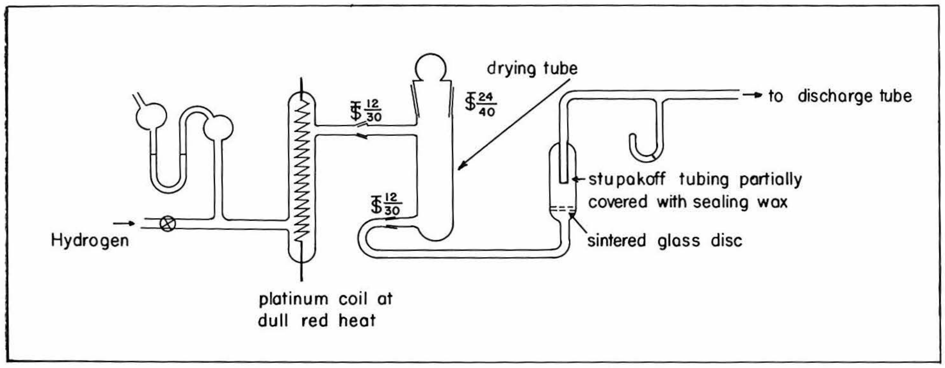

Figure 18. Hydrogen purifying train for hydrogen-discharge tube

by coating the surface of the tubing with sealing wax until the proper rate of flow was obtained.

The discharge tube operated at 1000 volts d-c with a current of 220 milliamperes. The tube was cooled with tap water during operation.

Discharge tube - absorption cell - The discharge tube - absorption cell illustrated in Figure 19 was 200 cm in length and 2.5 cm in diameter. Quartz windows were sealed to the tube with deKhotinsky cement. Precaution was taken to prevent any cement from entering the tube. The electrodes were aluminum cylinders 1.7 cm in diameter by 6 cm in length. The intake system consisted of a porous plate followed by a short piece of unglazed porcelain sealed directly to pyrex tubing and partially covered by a melt of sodium carbonate and borax to reduce the porosity. The leak was fitted with a by-pass closed with a stopcock so that the system could be swept out quickly. The sulfur dioxide entered at both ends of the tube and was withdrawn at the center. In this manner the fogging of the windows by the sulfur formed in the discharge was reduced. The oil pump on the exit line was protected by a double trap immersed in liquid air.

The shutter consisted of a circular metal disc containing four circular openings spaced 90° apart near the edge of the disc. The shutter was rotated by a 1800-rpm Bodine synchronous motor mounted between the absorption cell and spectrograph. By rotating the motor the openings in the shutter could be brought opposite

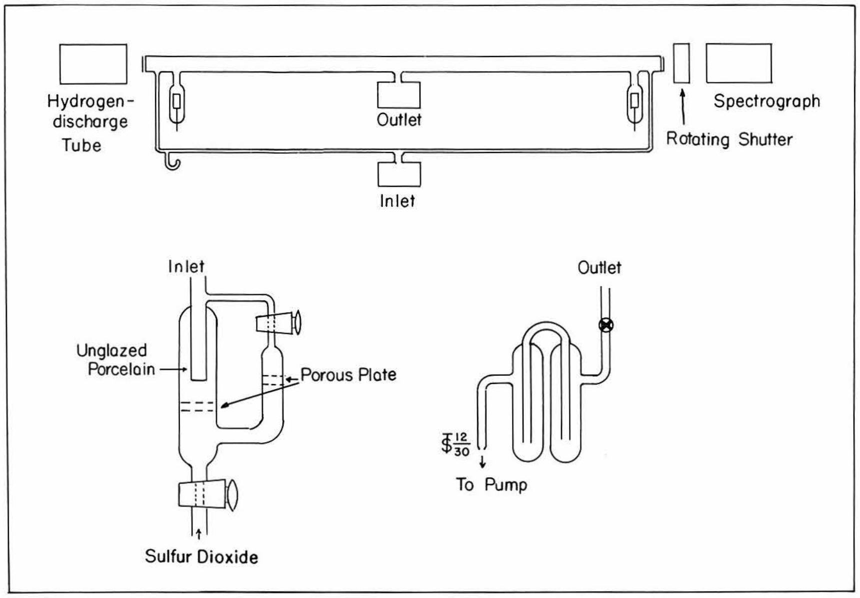

Figure 19. Combined absorption cell - discharge tube for "sulfur monoxide" investigation

the cell window at the two periods in the cycle when the discharge through the sulfur dioxide was off.

All spectra were recorded on Eastman "33" plates with a Bausch and Lomb Littrow Spectrograph, No. 269.

Schenk did not specify whether a condensed or uncondensed discharge was employed. Attempts to use an uncondensed discharge in the present experiment were without success. At gas pressures in which a discharge could be maintained, it was found that the discharge started too soon after the voltage passed through zero. The tube was not dark over the entire period during which the openings in the shutter were opposite the cell window, and no exposures were obtained which were entirely free of SO emission bands. When a 3.6×10^{-3} microfarad condenser was inserted in the electrical circuit, a discharge could easily be produced in the sulfur dioxide at a pressure of ~2 mm with a 12000 volt Thordarsen 1 KVA transformer. With a condensed discharge the cell remained dark for a sufficiently long fraction of each cycle to permit the absorption spectrum to be taken. The primary of the transformer was regulated by an 18 ampere, 0-130 volt Variac.

<u>Results</u> - Exposures were taken in sets of two. Each set contained one exposure taken of the discharge through the sulfur dioxide when the hydrogen discharge tube and rotating shutter were not in operation. This exposure showed the emission bands of SO partly obscured by sulfur dioxide absorption bands. In the second exposure the hydrogen tube and the shutter as well as the sulfur dioxide

discharge tube were in operation. In all exposures taken in this manner only the absorption spectrum of sulfur dioxide was observed. Thus, the "Schenk Bands" did not appear under conditions which yielded an intense SO emission spectrum.

Afterglow - In experiments employing the rotating shutter, the SO emission bands were not observed. However, the continuous spectrum was more intense than in exposures in which the hydrogen tube alone was operating. Several exposures were taken with the discharge through sulfur dioxide and the rotating shutter in operation. It was found that there was an afterglow emitted by the discharge which exhibited a continuous spectrum. The carrier of this afterglow is unknown. However, Martin reported that a continuum accompanied the SO bands and that, in the presence of an uncondensed discharge, most of the intensity was found in the continuum. It may be that the afterglow continuum observed here has the same carrier as the continuum observed by Martin.

(b) Production of the "Schenk Bands"

Modified discharge tube - Schenk had reported that the new absorption spectrum could be produced by passing sulfur dioxide alone through a discharge drawing 0.3 ampere at 3000 volts. Since no success was obtained in the present experiment with a 1 KVA transformer, an effort was made to duplicate the experimental conditions employed by Schenk. The system illustrated in Figure 20 was constructed to accommodate the increase in power and to closely

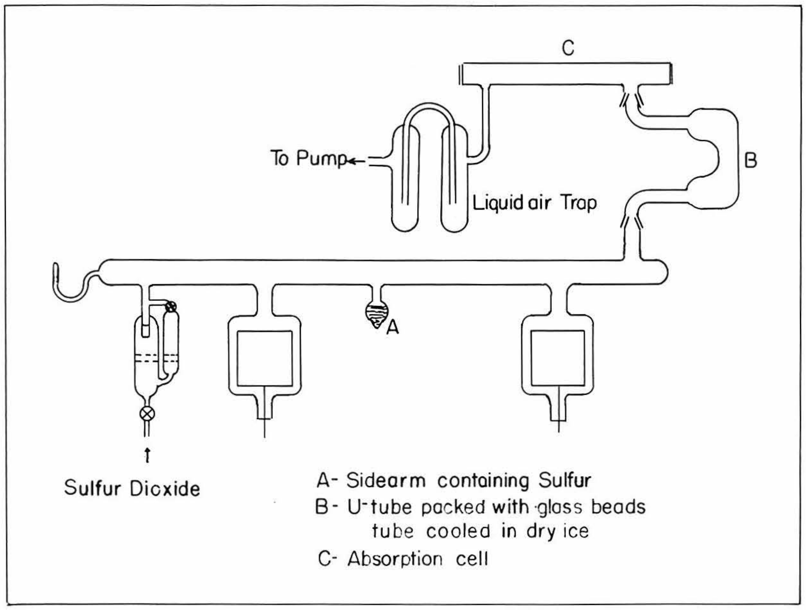

Figure 20. Discharge tube and absorption cell for the production of the "Schenk Bands"

resemble the apparatus reported by Schenk. Although Schenk stated that it was necessary to heat the electrodes during the experiment, it was found imperative in the present investigation to immerse the electrodes in oil baths to keep them from over-heating.

The voltage applied to the primary of a 9000 volt-10 KVA power transformer was controlled by a 220 volt-45 ampere Variac and a large inductance acting as an autotransformer. The inductance was tapped to give about 120 volts to the primary of the large transformer when the Variac was at full scale. The use of a step-down transformer permitted sufficient power to be brought through the 35 ampere fuses in the main power lines.

The secondary of the power transformer contained a 0-2 ampere a-c ammeter and 4500 ohms resistance in series with the discharge tube. Both sides of the ammeter were fused with 1-ampere fuses.

<u>Starting the discharge</u> - Due to the comparatively high pressure (5 to 10 mm) in the system, it was difficult to start the discharge. Consequently, the discharge was started at low pressure (below 2 mm). The pressure was gradually increased simultaneously with the output voltage of the transformer. With the discharge operating at gas pressures between 5 to 10 mm, the observed current in the secondary circuit was 0.4 to 0.7 amperes.

Numerous attempts were made at various pressures and discharge conditions to produce the "Schenk Bands" by passing sulfur dioxide alone through the discharge. At no time were absorption bands other than those due to sulfur dioxide observed.

Addition of sulfur vapor - The next modification was the addition of sulfur vapor to the sulfur dioxide stream. A few grams of flowers of sulfur were placed in a bulb and sealed into the system at "A" as indicated in Figure 19. The sulfur was vaporized by gently heating the bulb with a Bunsen burner. The addition of sulfur vapor to the discharge resulted in the immediate production of the absorption bands described by Schenk. In subsequent experiments the "Schenk Bands" were observed when oxygen and sulfur or air and sulfur were passed through the discharge. Reproductions of microphotometer tracings of the "Schenk Bands" as well as the sulfur dioxide spectrum are given in Figure 21.

(c) Confirmation that oxygen is necessary for the production of the "Schenk Bands"

Previous work - Earlier in this investigation it was shown that the "Schenk Bands" were not observed under conditions in which the known SO emission bands were strongly developed. Also, it is to be remembered that Cordes (66) had concluded that the "Schenk Bands" were due to an S_2^* molecule. Schenk had countered Cordes' proposal by pointing out that the spectrum persisted for several days when the gas was sealed at low pressure in carefully baked-out vessels and, therefore, the metastable molecule would have to possess an improbably long half-life. Schenk also performed the following experiment. The entire system was evacuated and the flow of sulfur dioxide stopped. Sulfur was then vaporized into the discharge tube and a discharge started. Absorption spectra of the sulfur vapor

Figure 21. Effect of temperature upon the "Schenk Bands". The lowest curve in each set is the result of subtracting the microphotometer trace of the sulfur dioxide bands from that of the sulfur dioxide - "Schenk Bands" mixture.

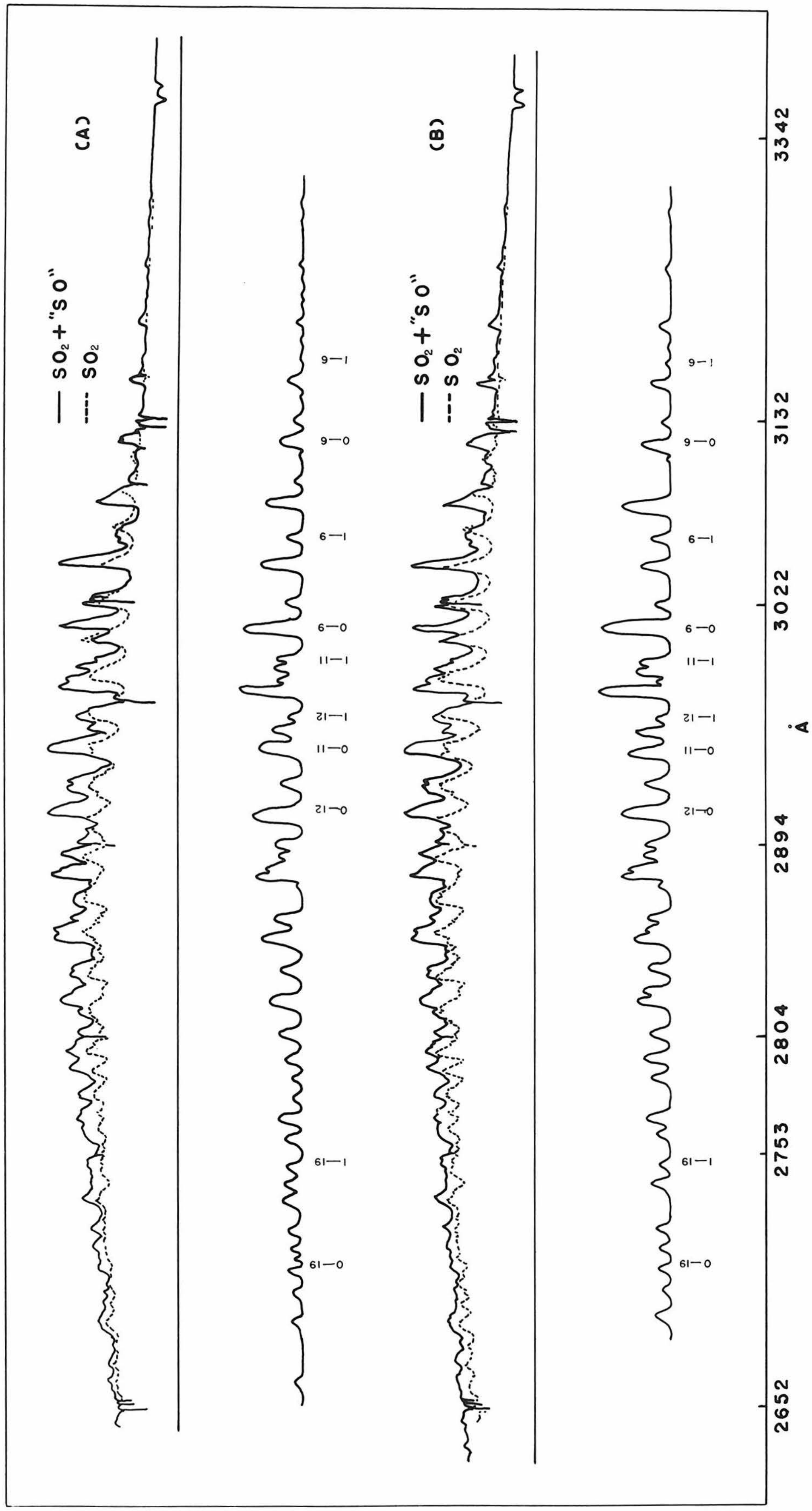
(A)
(B)
— SO_2+"SO"
--- SO_2
1—6
0—6
1—9
0—9
1—11
1—12
0—11
0—12
1—19
0—19
2652
2753
2804
2894
3022
3132
3342
Å

which had passed through the discharge were taken at suitable time intervals while the system was being continuously evacuated. It was reported that the intensity of the "Schenk Bands" decreased as the discharge continued and finally disappeared. Schenk interpreted this to indicate that the residual oxygen in the system was gradually used up and that the exhaustion of the oxygen coincided with the disappearance of the absorption bands. He concluded that oxygen was necessary for the production of the spectrum and that Cordes' interpretation was in error.

Present work - The experiment reported by Schenk could be criticized because the experimental conditions were not identical in the two cases. When the absorption bands were observed, gas was flowing continuously through the system; but, when the bands were observed to decrease in intensity, the system was closed except for sulfur vapor. A more direct approach is to pass oxygen and an inert gas plus sulfur into the discharge and then remove the oxygen from the gas stream. If the "Schenk Bands" appear in the first instance and not in the second, it would seem to be conclusive that oxygen is necessary for the production of the spectrum. This experiment was undertaken and its description follows.

Since no absorption bands other than those due to sulfur dioxide and the Schenk compound were observed when a mixture of oxygen, nitrogen, and sulfur was passed through the discharge, it was concluded that nitrogen would be satisfactory as an inert carrier gas. However, commercial tank nitrogen was observed to contain enough oxygen to yield the "Schenk Bands" when passed through the discharge tube with sulfur vapor. The oxygen was removed from the nitrogen by passing the gas stream over copper turnings held at red heat. The purifying train consisted of a trap immersed in liquid air to condense water, a quartz combustion tube containing copper turnings, and another trap immersed in liquid air to confine any condensable material which passed the first trap or was produced in the combustion tube. About 25 cm of the combustion tube was at red heat, and the copper turnings extended for 10 cm on either side of the heated area. Tygon tubing connected the various units of the purifying train.

Results - In a typical experiment the purifying train was allowed to run for 8 hours before an exposure was taken. This exposure showed no trace of the "Schenk Bands" or sulfur dioxide. When the copper furnace was by-passed and oxygen added to the nitrogen stream, the exposure showed both "Schenk Bands" and sulfur dioxide bands strongly. This observation substantiates that of Schenk and clearly indicates that oxygen is necessary for the production of the spectrum.

(d) Search for a temperature effect in the "Schenk Bands"

Expected temperature effect in "Schenk Bands" - Although Cordes appears to be in error in regard to the carrier of the observed bands, this does not necessarily invalidate his analysis of the spectrum in which he concluded that the value of the vibrational quantum in the ground state was 560 cm^{-1}. Using this value of 560 cm^{-1} for the vibrational quantum to calculate the population of the various excited levels as a function of temperature, it is found that the number of molecules in the first excited state at 300° K should be about four times that in the same state at 200° K. Therefore, the intensity of absorption bands originating from the first excited state should increase by a factor of four when the temperature of the gas is increased from 200° K to 300° K.

Experimental - A cell 40 cm in length was constructed from 42 mm O.D. tubing drawn down to accommodate 25-mm quartz windows at each end. A thermocouple well was inserted just inside the large diameter portion of the cell to a length of 15 cm. A chromel-alumel thermocouple was connected directly to a microammeter. The thermocouple was calibrated with boiling water, freezing tin (232° C), and freezing zinc (420° C). The temperatures measured in this manner are accurate to within ± 2°.

For the low-temperature exposure the cell was packed in dry ice to within a distance of not less than 2 cm from each end in order to avoid the condensation of atmospheric moisture on the windows. Thus, at the low temperature only slightly more than 35 cm of the 40-cm cell was actually at the temperature of subliming carbon dioxide.

Results - Since the gas stream contained both sulfur dioxide and the unidentified absorber, it was necessary to determine the absorption due to the "Schenk Bands" alone before any temperature effects could be ascertained. Therefore, absorption spectra were taken of the gas stream as well as exposures of the spectrum of sulfur dioxide alone with the cell at room temperature and with the cell packed in dry ice. Enlarged projections of microphotometer traces of plates containing both spectra taken at each temperature were superimposed upon similar projections of exposures containing only sulfur dioxide. In principle, by subtracting the curve representing the intensity of the sulfur dioxide bands from that of the mixture, the absorption due to the unknown substance alone can be obtained. This was done for several exposures at both temperatures as illustrated in Figure 21. The absorption peaks are numbered in accordance with Cordes' analysis (66).

The population of the excited vibrational levels increases significantly with increase in temperature, but the relative decrease in population of the ground vibrational level is small. Therefore, the intensity of absorption bands originating from excited vibrational levels will increase with increase in temperature, whereas, the intensity of bands involving transitions from the ground state will be essentially unaffected by changes of a few hundred degrees in temperature. Thus, the observed intensities of bands originating from the first vibrational level can be referred to the intensities of the corresponding bands originating from the ground vibrational level. As the temperature increases the value of $I_{0 \rightarrow v'}/I_{1 \rightarrow v'}$ decreases. Table 27 contains the observed intensity ratio at two temperatures for various values of v'. Results from two sets of traces are contained in the table.

Table 27

Observed Intensity Ratios for Several Pairs of "Schenk Bands"

	Intensity Ratio			
	200° C		300° C	
Bands	Set A	Set B	Set A	Set B
0-6/1-6	5.0	6.0	6.7	9.0
0-8/1-8	2.5		4.8	4.7
0-9/1-9	2.8		5.2	3.9
0-11/1-11	1.4	1.4	1.9	1.7
0-12/1-12	3.6	3.3	2.7	3.5
0-13/1-13	4.0	1.6	3.6	2.2
0-19/1-19	1.5	1.1	1.1	1.0

The observed intensity ratios do not show an average decrease as the temperature increases. On the contrary, if there is any temperature effect, it appears to be a small one in the opposite direction. No temperature effect was detected for any of the "Schenk Bands".

Since the process of subtraction of the two microphotometer traces is somewhat arbitrary, it is difficult to determine how far the resulting intensity curve deviates from the actual absorption curve of the unknown substance. However, that some confidence can be placed in the method is indicated by the general agreement between measurements made on two sets of traces at the same temperature.

3. Conclusions

The present spectroscopic investigation of the absorption bands described by Schenk yielded little new information concerning the carrier of this spectrum. However, it was possible to substantiate some previously reported observations.

Kornfeld and McCaig (72) had been unable to observe any new absorption bands in sulfur dioxide after it had passed through an electrodeless discharge, although the emission bands of SO were observed in the discharge. In the present investigation a similar experiment yielded no detectable absorption other than that of sulfur dioxide when the latter gas was passed through a discharge between aluminum electrodes. Even with power levels and pressures equal to and greater than those reported by Schenk, the new bands could not be produced in sulfur dioxide alone. On the other hand, when sulfur vapor was introduced into the gas stream which consisted of sulfur dioxide, oxygen, or oxygen and nitrogen, the "Schenk Bands" were readily observed in the stream after it had passed through the discharge.

Schenk's contention that the presence of oxygen in some form is necessary for the production of the spectrum has been corroborated. In the experiment described here the conditions of the discharge were held constant and the amount of oxygen in the gas stream was varied. The "Schenk Bands" were observed only when oxygen was passing through the discharge. It may now be concluded that Cordes' suggestion that the new spectrum is due to an activated sulfur molecule is untenable.

If the population of the excited vibrational levels were sufficiently large and could be altered appreciably by reasonable changes in temperature, the "Schenk Bands" would show a temperature effect. Using 560 cm^{-1} as the vibrational quantum in the ground state, as suggested by Cordes, it was calculated that the population of the first vibrational level could be increased by nearly a factor of four by changing the temperature from 200 K to 300 K. No temperature effect could be detected in the "Schenk Bands" over this temperature range. Since it was necessary to subtract the absorption due to sulfur dioxide from the observed absorption of the mixture, the values obtained for the "Schenk Bands" may be seriously in error. Therefore, this apparent lack of temperature dependence cannot be taken as conclusive evidence that the analysis of Cordes is incorrect.

Several experiments not detailed above may be mentioned here. It was, indeed, found possible to produce the new spectrum by burning sulfur in oxygen at pressures of about 15 mm as reported by Schenk. However, this method did not produce condensable quantities of the new material and the large amounts of sulfur vapor produced rapidly fogged the cell windows and clogged the system.

An attempt was made to produce the "Schenk Bands" by passing sulfur dioxide alone, or combined with sulfur vapor, through a Siemen's type ozonizer. The "Schenk Bands" were not observed, but in one instance droplets of orange liquid were seen in the ozonizer. This material decomposed rapidly with some effervescence to yield what appeared to be sulfur. It may well be that this condensate was similar to that identified by Schenk as a polymerized form of the material yielding the absorption spectrum.

Appendix. Derivation of Expressions for the Three Principal Moments of Inertia for a Non-linear, Non-planar, X_2Y_2 Molecule

Appendix. Derivation of Expressions for the Three Principal Moments of Inertia for a Non-linear, Non-planar, X Y Molecule

First, consider a planar-cis configuration,

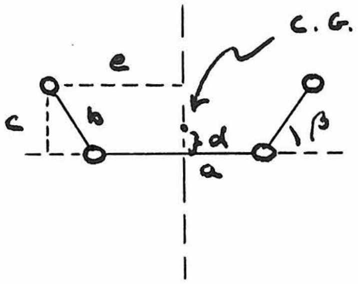

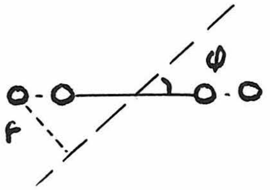

where a = X-X bond distance

b = X-Y bond distance

Pass a plane through the center of gravity, perpendicular to the Y-X-X plane, and parallel to the X-X bond. It is desired to find the moment of inertia about any axis lying in this plane and passing through the center of gravity. The angle this axis makes with the intersection of the two planes is designated by φ.

Then it is easily seen that

$$c = b \text{ Sin } \beta$$

$$d = b \text{ Sin } \beta \,/(M_X/M_Y)$$

$$e = b \text{ Cos } \beta$$

$$f = e \text{ Sin } \varphi$$

Let l_X = perpendicular distance from axis to X atoms

If $\phi = 90^\circ$

$$l_X^2 = (a/2)^2 + d^2$$

Or for any value of ϕ

$$l_X^2 = (a/2 \text{ Sin } \phi)^2 + d^2$$

Let l_Y = perpendicular distance from axis to Y atoms

If $\phi = 90^\circ$

$$l_Y^2 = e^2 + (c-d)^2$$

Or for any value of ϕ

$$l_Y^2 = (e \text{ Sin } \phi)^2 + (c-d)^2$$

Now consider a non-planar model

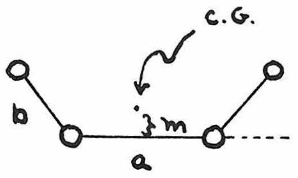

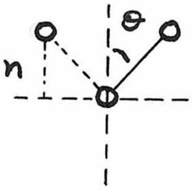

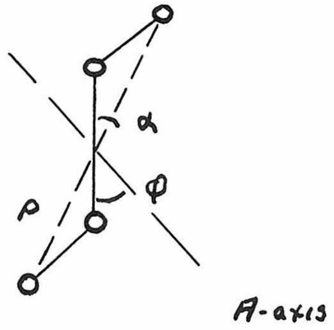

Then

$$n = c \text{ Cos } \theta$$

$$m = c \text{ Cos } \theta / (M_X/M_Y)$$

$$\alpha = \text{Tan}^{-1} (c \text{ Sin } \theta / e)$$

$$p^2 = (e)^2 + (c \text{ Sin } \theta)^2$$

where, in the plane containing the A-axis, α is the angle between the projection of the X-X bond and a line joining the two Y atoms, θ is the half-angle between the two Y-X-X planes, p is one-half the distance between the two Y atoms, and c and e have the same meaning as in the planar model.

Let ℓ_Y = perpendicular distance from A-axis to Y atoms

If $\phi = 90^\circ - \alpha$

$$\ell_Y^2 = p^2 + (n-m)^2$$

If $\phi = 90^\circ$

$$\ell_Y^2 = (p \operatorname{Cos} \alpha)^2 + (n-m)^2$$

Or for any value of ϕ

$$\ell_Y^2 = (n-m)^2 + (p \operatorname{Sin}(\phi + \alpha))^2$$

Let ℓ_X = perpendicular distance from A-axis to X atoms

$$\ell_X^2 = m^2 + ((a/2) \operatorname{Sin} \phi)^2$$

By definition

$$I = \sum m_i \ell_i^2$$

therefore

$$I_A = 2M_Y \left[(n-m)^2 + p^2 \operatorname{Sin}^2(\alpha + \phi_A) \right] + 2M_X \left[m^2 + (a^2/4) \operatorname{Sin}^2 \phi_A) \right]$$

In a similar manner we find

$$I_B = 2M_Y \left[(n-m)^2 + p^2 \operatorname{Sin}^2(90^\circ - (\alpha + \phi_A)) \right] + 2M_X \left[m^2 + (a^2/4) \operatorname{Sin}^2(90^\circ - \phi_A) \right]$$

$$I_C = 2M_Y p^2 + 2M_X (a/2)^2$$

where, the C-axis is the symmetry axis of the molecule, the B-axis is at right angles to the A and C axes, and ϕ_A is the value of ϕ which makes I_A a minimum.

To make the A-axis the axis of least inertia we minimize I_A with respect to ϕ.

Note that n, m, p, and α do not depend on ϕ.

$$I_A = 2M_Y\left[(n-m)^2 + p^2 \mathrm{Sin}^2(\phi+\alpha)\right] + 2M_X\left[m^2 + (a^2/4)\ \mathrm{Sin}^2\phi\right]$$

$$dI_A/d\phi = 2M_Y(2)p^2\ \mathrm{Sin}(\phi+\alpha)\mathrm{Cos}(\phi+\alpha) + 2M_X(a^2/4)2\mathrm{Sin}\,\phi\,\mathrm{Cos}\,\phi$$

Equating to zero

$$4M_Y p^2 \mathrm{Sin}(\phi+\alpha)\mathrm{Cos}(\phi+\alpha) + M_X a^2 \mathrm{Sin}\,\phi\,\mathrm{Cos}\,\phi = 0$$

Substitute

$$\mathrm{Sin}\ 2x = 2\mathrm{Sin}\ x\ \mathrm{Cos}\ x$$

Then

$$2M_Y p^2 \mathrm{Sin}(2\phi + 2\alpha) + (M_X a^2/2)\mathrm{Sin}\ 2\phi = 0$$

But

$$\mathrm{Sin}(x+y) = \mathrm{Sin}\ x\ \mathrm{Cos}\ y + \mathrm{Cos}\ x\ \mathrm{Sin}\ y$$

Then

$$4M_Y p^2\left[\mathrm{Sin}\ 2\phi\ \mathrm{Cos}\ 2\alpha + \mathrm{Cos}\ 2\phi\ \mathrm{Sin}\ 2\alpha\right] + M_X a^2 \mathrm{Sin}\ 2\phi = 0$$

Now substituting $\mathrm{Cos}\ 2\phi = (1-\mathrm{Sin}\ 2\phi)^{-1/2}$, squaring, and solving for Sin 2ϕ we obtain

$$\mathrm{Sin}\ 2\phi = \frac{4\ M_Y\ p^2\ \mathrm{Sin}\ 2\alpha}{(16\ M_Y^2\ p^4 + M_X^2\ a^4 + 8\ M_X M_Y\ a^2 p^2\ \mathrm{Cos}\ 2\alpha)^{1/2}}$$

for the value of ϕ which makes I_A a minimum.

References

References

1. S. L. Gerhardt, Phys. Rev. 42, 622 (1932)
2. G. Hettner, R. Pohlmann, and H. J. Schumacher, Zeits. f. Physik 91, 372 (1934)
3. W. G. Penney and G. B. B. M. Sutherland, Proc. Roy. Soc. A156, 654 (1936)
4. D. M. Simpson, Trans. Faraday Soc. 41, 209 (1945)
5. A. Adel and D. M. Dennison, J. Chem. Phys. 14, 379 (1946)
6. W. Shand and R. A. Spurr, J. Am. Chem. Soc. 65, 179 (1943)
7. H. Johnston, Ph.D. Thesis, Calif. Inst. of Tech. (1947)
8. See, for example, J. F. Schultz and O. R. Wulf, J. Am. Chem. Soc. 62, 2980 (1940)
9. F. P. Treadwell and W. T. Hall, "Analytical Chemistry," Vol. II, p. 573 (John Wiley and Sons, Inc., New York, 1928)
10. E. B. Wilson, Jr. and A. J. Wells, J. Chem. Phys. 14, 578 (1946)
11. E. Bartholomè, Zeits. f. physik. Chemie B23, 131 (1933)
12. D. M. Simpson, J. Chem. Phys. 15, 846 (1947)
13. B. Lewis and G. von Elbe, J. Chem. Phys. 2, 294 (1934)
14. L. Lefebvre, Comptes rendus 199, 456 (1934)
15. A. Yakovleva and V. Kondrat'eva, Phys. Zeits. Sovejetunion 9, 106 (1936)
16. W. H. Eberhardt and W. Shand, J. Chem. Phys. 14, 525 (1946)
17. G. Herzberg, "Infrared and Raman Spectra of Polyatomic Molecules," p. 284 (D. Van Nostrand Co. Inc., New York, 1945)
18. L. Harris, W. S. Benedict, and G. W. King, Nature 131, 621 (1931)

19. S. Claesson, J. Donohue, and V. Schomaker, J. Chem. Phys. 16, 207 (1948)

20. R. Schaffert, J. Chem. Phys. 1, 507 (1933)

21. L. Harris and G. W. King, J. Chem. Phys. 2, 51 (1934)

22. G. B. B. M. Sutherland, Proc. Roy. Soc. 145, 278 (1934)

23. G. B. B. M. Sutherland, Proc. Roy. Soc. 141, 342 (1933)

24. L. Pauling, "Nature of the Chemical Bond," p. 271 (Cornell University Press, Ithaca, N.Y., 1941)

25. D. M. Yost and Horace Russell, Jr., "Systematic Inorganic Chemistry," p. 28 (Prentice-Hall, Inc., New York, 1944)

26. F. Verhoek and F. Daniels, J. Am. Chem. Soc. 53, 1250 (1931)

27. G. N. Lewis and M. Randall, "Thermodynamics and the Free Energy of Chemical Substances," p. 561 (McGraw-Hill, Inc., New York, 1923)

28. D. Williams and L. Derchard, J. Am. Chem. Soc. 61, 1382 (1939)

29. R. Rollefson and R. Havens, Phys. Rev. 57, 710 (1940)

30. A. M. Thorndike, J. Chem. Phys. 15, 868 (1947)

31. A. M. Thorndike, A. J. Wells, and E. Bright Wilson, Jr., J. Chem. Phys. 15, 157 (1947)

32. E. Bright Wilson, Jr. and A. J. Wells, J. Chem. Phys. 14, 578 (1946)

33. T-Y. Wu, "Vibrational Spectra and Structure of Polyatomic Molecules," p. 273 (J. W. Edwards, Ann Arbor, Mich., 1946)

34. H. Boersch, Acad. Wiss. Wien 11b, 144, 1 (1935)

35. H. Boersch, Monatsh. 65, 311 (1935)

36. L. E. Sutton and L. O. Brockway, J. Am. Chem. Soc. 57, 473 (1935)

37. G. Hettner, R. Pohlmann, and H. J. Schumacher, Zeits. f. Physik 96, 203 (1935)

38. P. Lebeau and A. Damiens, Comptes rendus 188, 1253 (1928)

39. G. B. B. M. Sutherland and W. G. Penney, Proc. Roy. Soc. 156, 678 (1936)

40. C. R. Bailey, J. B. Hale, and J. W. Thompson, Proc. Roy. Soc. 167, 555 (1938)

41. D. M. Yost, E. N. Lassettre, and S. T. Gross, J. Chem. Phys. 4, 325 (1936)

42. G. Herzberg, "Infrared and Raman Spectra of Polyatomic Molecules," p. 285 (D. Van Nostrand Co. Inc., New York, 1945)

43. V. Schomaker and D. P. Stevenson, J. Am. Chem. Soc. 62, 1267 (1940)

44. G. Herzberg, "Infrared and Raman Spectra of Polyatomic Molecules," p. 187 (D. Van Nostrand Co. Inc., New York, 1945)

45. C. R. Bailey and A. B. D. Cassie, Proc. Roy. Soc. 142, 129 (1933)

46. F. L. Usher, J. Chem. Soc. 127, 730 (1925)

47. D. M. Yost and Horace Russell, Jr., "Systematic Inorganic Chemistry," p. 41 (Prentice-Hall, Inc., New York, 1944)

48. G. Herzberg, "Infrared and Raman Spectra of Polyatomic Molecules," p. 301 (D. Van Nostrand Co. Inc., New York, 1945)

49. K. H. Butler and O. Maass, J. Am. Chem. Soc. 52, 2184 (1930)

50. D. P. Stevenson and J. Y. Beach, J. Am. Chem. Soc. 60, 2872 (1938)

51. W. G. Penney and G. B. B. M. Sutherland, J. Chem. Phys. 2, 492 (1934)

52. L. R. Zumwalt and P. A. Giguère, J. Chem. Phys. 9, 458 (1941)

53. R. M. Badger, L. R. Zumwalt, and P. A. Giguère, Rev. of Sci. Insts. (in press)

54. L. Pauling, "Nature of the Chemical Bond," p. 164 (Cornell University Press, Ithaca, N.Y., 1942)

55. P. G. Ackermann and J. E. Mayer, J. Chem. Phys. 4, 377 (1936)

56. K. J. Palmer, J. Am. Chem. Soc. 60, 2360 (1938)

57. G. Herzberg, "Infrared and Raman Spectra of Polyatomic Molecules," p. 283 (D. Van Nostrand Co. Inc., New York, 1945)

58. C. R. Bailey and R. R. Gordon, Trans. Faraday Soc. 34, 1133 (1938)

59. G. Herzberg, "Molecular Spectra and Molecular Structure," Vol. I, Table 36 (Prentice-Hall, Inc., New York, 1939)

60. P. Krishnamurti, Indian J. of Phys. 5, 105 (1930)

61. Y. Morino and S. Mizushima, Scient. Pap. Inst. Phys. Chem. Res. (Tokyo) 32, 220 (1937)

62. G. Herzberg "Infrared and Raman Spectra of Polyatomic Molecules," p. 435 (D. Van Nostrand Co. Inc., New York, 1945)

63. G. Herzberg "Infrared and Raman Spectra of Polyatomic Molecules," p. 489 (D. Van Nostrand Co. Inc., New York, 1945)

64. P. W. Schenk, Z. anorg. allg. Chem. 211, 150-160 (1933)

65. a. H. Cordes and P. W. Schenk, Z. Electrochem. 39, 594-596 (1933)
    b. H. Cordes and P. W. Schenk, Z. anorg. allg. Chem. 214, 33-43 (1933)
    c. P. W. Schenk and H. Platz, ibid., 215, 113-128 (1933)
    d. P. W. Schenk, ibid., 220, 268-272 (1934)
    e. H. Cordes and P. W. Schenk, Trans. Faraday Soc. 30, 31-33 (1934)
    f. P. W. Schenk and H. Platz, Z. anorg. allg. Chem. 222, 177-188 (1935)
    g. P. W. Schenk and H. Triebel, ibid., 229, 305-312 (1936)
    h. P. W. Schenk, Z. f. Physik 106, 271-272 (1937)
    i. P. W. Schenk, Z. anorg. allg. Chem. 233, 385-400 (1937)
    j. P. W. Schenk, Z. Electrochem. 47, 855 (1941)
    k. P. W. Schenk, Z. physik. Chem. B51, 113-119 (1942)
    l. P. W. Schenk, ibid., B52, 295-298 (1942)

66. H. Cordes, Z. f. Physik 105, 251 (1937)

67. A. Yakovleva and V. Kondrat'eva, Acta Physicochim. U.R.S.S. 241 (1940)

68. V. Kondrat'eva and E. Kondrat'eva, J. Chem. Phys. (U.S.S.R.) <u>14</u>, 1528 (1940)

69. E. Kondrat'eva and V. Kondrat'eva, J. Chem. Phys. (U.S.S.R.) <u>15</u>, 731 (1942)

70. E. V. Martin, Phys. Rev. <u>41</u>, 167 (1932)

71. R. M. Badger, J. Chem. Phys. <u>2</u>, 128 (1934); <u>3</u>, 710 (1935)

72. G. Kornfeld and M. McCaig, Nature <u>135</u>, 185 (1935)

Propositions

Propositions

1. No banded spectrum involving the ground state of fluorine is known. It is proposed that the use of an electrodeless discharge through fluorine may permit a banded spectrum to be observed.

2. With the usual chromatographic arrangement in which the filtrate is allowed to accumulate in a suction flask it is necessary to halt development and release the suction each time the receiver is to be changed. However, this operation is time-consuming, and in many chromatographic separations the interruption of the chromatogram may lead to considerable distortion and subsequent poor separation of the zones when development is resumed. An all-glass adaptor has been constructed which allows the chromatographer to change receivers rapidly and as frequently as is necessary during a chromatogram without discontinuing development or releasing the suction on the column at any time.

3. It is proposed that an investigation of the vibration spectrum of deuterium fluoride would be of interest, since the 0 - 3 band of hydrogen fluoride shows a reversal in the R branch (1). Also, the determination of D (DF) would be of interest in connection with the dissociation energy of fluorine.

(1) D. E. Kirkpatrick and E. O. Salant, Phys. Rev. 48, 945 (1935)

4. There is disagreement concerning the constitution of the lower sulfur fluorides. It is suggested that an infrared investigation of the gaseous material could be of aid in this problem.

5. The application of Badger's Rule (1) to the interhalogen compounds indicates that Herzberg's value (2) for the vibrational quantum of BrCl is too low.

(1) R. M. Badger, J. Chem. Phys. 2, 128 (1934); 3, 710 (1935)

(2) G. Herzberg, "Molecular Spectra and Molecular Structure," Vol. I, p. 484 (Prentice-Hall, Inc., New York, 1939)

6. (a) An acidic solution of tetravalent cerium is a superior streak reagent for the detection of certain N-substituted aniline derivatives on chromatographic columns.

(b) A sulfuric acid solution of tetravalent cerium slowly deteriorates but a phosphoric acid solution does not. An explanation can be given for this phenomenon.

7. Daly and Sutherland (1) recently suggested a method for obtaining "instantaneous" spectra. It is proposed that the use of a lead sulfide detector and the cathode-ray tube described by Johnson (2) would extend the usefulness of this technique.

(1) E. F. Daly and G. B. B. M. Sutherland, Nature <u>157</u>, 547 (1946)
(2) J. B. Johnson, J. App. Phys. <u>17</u>, 891 (1946)

8. Dr. Oliver R. Wulf (1) has suggested that the carrier of the "Schenk Bands" (2) may be a sulfur analogue to ozone, such as S_2O. This possibility could be investigated by allowing the unidentified substance to react with various gaseous olefins.

(1) Private communication
(2) This Thesis, Part III

9. The vibration spectrum of chlorine monoxide has been investigated by Bailey and Cassie (1). A new vibrational assignment can be made which is in agreement with the assignments found for ozone and oxygen fluoride (2).

(1) C. R. Bailey and A. B. D. Cassie, Proc. Roy. Soc. <u>142</u>, 129 (1933)
(2) This Thesis, Part I

10. Both liquid and solid nitric oxide are blue (1). It is suggested that authors of inorganic text books should take cognizance of this well established fact (2).

(1) H. L. Johnston and W. F. Giauque, J. Am. Chem. Soc. <u>51</u>, 3194 (1929)
(2) See, for example, F. Ephraim, "Inorganic Chemistry," p. 673 (Interscience Pub. Inc., New York, 1946); J. W. Mellor, "Mellor's Modern Inorganic Chemistry," p. 417 (Longmans, Green and Co., New York, 1939)